remote sensing

MDPI

Article

Drought Disasters in China from 1991 to 2018: Analysis of Spatiotemporal Trends and Characteristics

Xiaofeng Wang [1,2,3], Pingping Luo [1,2,3,*], Yue Zheng [1,2,3], Weili Duan [4,*], Shuangtao Wang [1,2,3], Wei Zhu [1,2,3], Yuzhu Zhang [5] and Daniel Nover [6]

1 Key Laboratory of Subsurface Hydrology and Ecological Effects in Arid Region, Ministry of Education, Chang'an University, Xi'an 710054, China
2 School of Water and Environment, Chang'an University, Xi'an 710054, China
3 Xi'an Monitoring, Modelling and Early Warning of Watershed Spatial Hydrology International Science and Technology Cooperation Base, Chang'an University, Xi'an 710054, China
4 State Key Laboratory of Desert and Oasis Ecology, Key Laboratory of Ecological Safety and Sustainable Development in Arid Lands, Xinjiang Institute of Ecology and Geography, Chinese Academy of Sciences, Urumqi 830011, China
5 Shaanxi Key Laboratory of Earth Surface System and Environmental Carrying Capacity, College of Urban and Environmental Sciences, Northwest University, Xi'an 710127, China
6 School of Engineering, University of California—Merced, 5200 Lake R, Merced, CA 95343, USA
* Correspondence: lpp@chd.edu.cn (P.L.); duanweili@ms.xjb.ac.cn (W.D.)

Abstract: Droughts have emerged as a global problem in contemporary societies. China suffers from different degrees of drought almost every year, with increasing drought severity each year. Droughts in China are seasonal and can severely impact crops. This study used spatiotemporal trend and characteristics analysis of drought disaster data from 1991 to 2018 in Chinese provinces, in addition to the Mann–Kendall test and wavelet analysis. The drought disaster data included the crop damage area, drought-affected area of the crops, and crop failure area. The outputs of the crops decreased by 10%, 30%, and 80%, respectively. The population with reduced drinking water caused by drought, and the domestic animals with reduced drinking water caused by drought, were numbered in the tens of thousands. The results of the study show that the crop damage areas owing to drought disasters, drought-affected areas of crops, and crop failure areas in China were mainly distributed in the northern, eastern, northeaster, and southwestern regions. The number of people and domestic animals with reduced drinking water owing to drought in China were mainly concentrated in the northern and southwestern regions. These indicators showed a general increasing trend. Tibet, Fujian, Shandong, Jiangsu, Anhui, and Henan provinces and autonomous regions also showed a slightly increasing trend. In particular, the number of domestic animals with reduced drinking water caused by drought in the Inner Mongolia Autonomous Region showed a clear increasing trend with a significant Z-value of 2.2629. The results of this research can be used to provide scientific evidence for predicting future trends in drought and for practising the best management of drought prevention and resistance.

Keywords: drought disaster; trend analysis; wavelet analysis; spatial distribution

Citation: Wang, X.; Luo, P.; Zheng, Y.; Duan, W.; Wang, S.; Zhu, W.; Zhang, Y.; Nover, D. Drought Disasters in China from 1991 to 2018: Analysis of Spatiotemporal Trends and Characteristics. *Remote Sens.* **2023**, *15*, 1708. https://doi.org/10.3390/rs15061708

Academic Editor: John J. Qu

Received: 30 November 2022
Revised: 8 January 2023
Accepted: 12 January 2023
Published: 22 March 2023

1. Introduction

Drought is considered to be the second largest natural disaster worldwide [1]. Although the frequency of droughts is relatively low, the resulting economic losses are very serious, accounting for almost 30% of the total economic losses for all natural disasters [2].

The most significant reduction factor in global agricultural production is no longer a simple ecological problem. Because droughts have a complex formation mechanism, long duration, wide range, high frequency, and high potential harm, they not only seriously affect agricultural production, but also directly affect social and economic development and stability, deteriorate people's living conditions, threaten global food security, and slow down the pace of world economic recovery [3]. China is one of the most drought-prone countries worldwide [4]. Drought has become the main natural force causing fluctuations in grain production, directly threatening national food security. Therefore, it is necessary to study drought disasters in China [5].

In recent years, experts and scholars worldwide have also considered drought disasters as an important field of research. Liu et al., based on a previous study, analysed the spatial anomaly characteristics and temporal variation of the standardised drought index based on monthly precipitation and average monthly temperature data from 589 meteorological stations in China from 1961 to 2009 using the empirical orthogonal function (EOF)/revolving empirical orthogonal function (REOF), wavelet transform, and Mann–Kendall mutation test [6]. Based on a previous study, Choi et al. compared the standard and remote sensing drought indices with water flow and soil moisture measurement data from 2000 to 2008 in a small experimental river basin in Georgia [7]. Many other scholars have used the meteorological drought composite index (MCI) [8], standardised precipitation evapotranspiration index (SPEIS) [9], vegetation condition index (VCI) [10], and standardised precipitation index (SPI) [11,12] methods to study drought indices [13]. The remote sensing technology they use provides a powerful means for the rapid and quantitative understanding of droughts [14]. However, the relationship between soil, water, and vegetation involved in drought is very complex, and it is still very difficult for remote sensing methods to restore real surface characteristics [15,16]. Luo et al. [17] studied drought hazard risk zoning, assessment, analysis, and management. Disaster situations have also been used by many scholars as indicators to study drought disasters, and results have been obtained using many different research methods. Statistical and comprehensive analysis methods were used by Jiang et al. to analyse the trends and causes of major meteorological disasters affecting agricultural production in China from 1995 to 2014 [18]. Statistical data from 1979 to 2008 were used by Fang et al. to analyse the temporal changes and spatial distribution characteristics of agrometeorological disasters in China over the past 30 years [19]. The temporal change trend and spatial distribution characteristics of drought and flood disasters in China were analysed by Yao et al. based on the statistical data of disaster areas of China from 1950 to 2010 [20]. Based on the M-K trend test and the M-K mutation test, Tian et al. analysed the trend in droughts in China's main grain-producing areas from 1949 to 2016, with the aim of reducing the risk of drought in the main grain-producing areas, and disaster loss measures provided a theoretical basis [21].

Most studies on droughts have focused on small regional, provincial, or national scales, whereas few studies have been conducted on drought hazards on a national scale, and fewer small-wave analyses of droughts have been conducted [22]. Therefore, this study used the M-K test and wavelet analysis to analyse the spatial and temporal trends, characteristics, and distribution of drought disasters in China. Specifically, this study analysed data on five items of agricultural drought disasters in 30 provinces from 2006 to 2017 (i.e., crop damage area, drought-affected area of crops, crop failure area, populations with reduced drinking water caused by drought, and domestic animals with reduced drinking water caused by drought). Data from five kinds of droughts in China from 1991 to 2018 were also analysed to describe the trends in agricultural droughts and the associated changes in socioeconomic losses in China. The temporal and spatial distribution characteristics of drought occurrence were obtained, and the evolution law of drought was clarified to provide theoretical support for the rational utilisation of water resources and the prevention of agricultural drought and agricultural production processes. The results of this study can provide a scientific reference for drought disaster prevention and mitigation.

2. Study Area, Data, and Methods

2.1. Study Area

As shown in Figure 1, China is a large country with a large population and a large land area. Therefore, the combination of temperature and precipitation in China is diverse and forms various climatic zones [23]. This results in an uneven distribution of precipitation, such that droughts and floods have obvious seasonal and regional variations [24]. Most areas north of Qinling and the Huaihe River experience spring droughts or continuous droughts in the spring and summer, followed by summer droughts, with continuous droughts in spring, summer, and autumn in some years [25]. South of the Qinling and Huaihe rivers to the Guangxi Zhuang Autonomous Region and the northern part of Guangdong Province, there are more droughts in autumn and fewer droughts in spring. There are many droughts in autumn and winter and in winter and spring in southern China [26]. In some years, there are continuous droughts in autumn, winter, and spring, but few droughts occur in the summer [27,28]. There are many winter droughts and spring droughts in the southwest, spring droughts and summer droughts often occur in north-western Sichuan Province, and autumn droughts often occur in eastern Sichuan Province [29]. China experiences frequent natural disasters, and the economic losses caused by meteorological disasters account for a large proportion of all disasters. Among these, the economic losses caused by drought disasters account for more than half of the meteorological disasters [30].

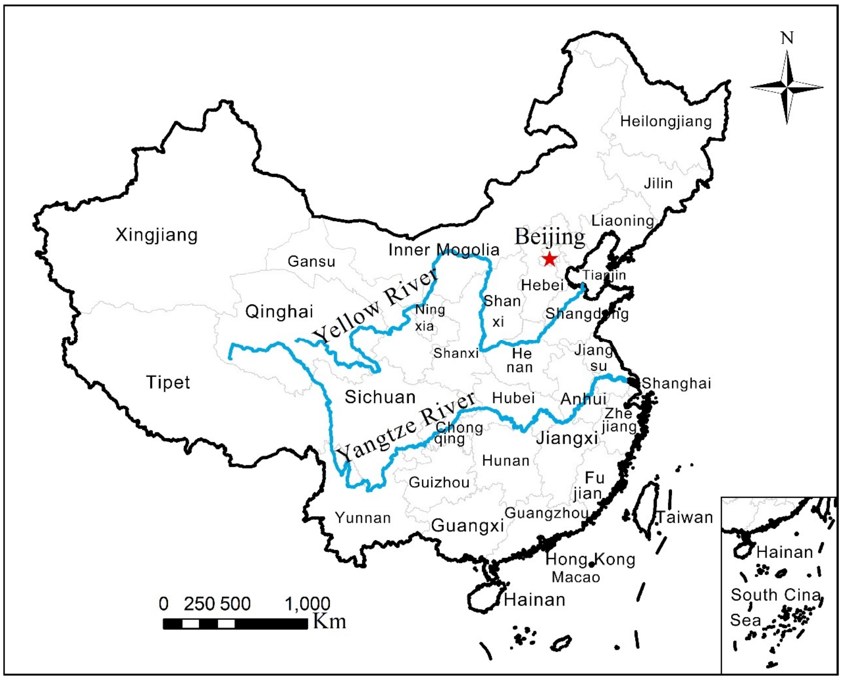

Figure 1. Administrative map of China.

2.2. Data Sources

First, we collected literature records, historical documents, government reports, and drought disaster data to understand the history and current status of drought studies around the world. The research goals and contents were determined by reading the documents and materials. After consulting the "Bulletin of Flood and Drought Disaster in China" [31], useful data were extracted and sorted.

The drought data in this study came from the drought disaster data in the "Bulletin of Flood and Drought Disaster in China" in recent years (http://www.mwr.gov.cn/sj/tjgb/zgshzhgb/ (accessed on 29 November 2022)). The period of drought disaster data for the provinces in China was from 2006 to 2017. The drought disaster data included five items: crop damage area (thousands of hectares), drought-affected area of crops (thousands of hectares), crop failure area (thousands of hectares), population with reduced drinking water caused by drought (tens of thousands), and domestic animals with reduced drinking water caused by drought (tens of thousands) [32]. From 1991 to 2018, the drought disaster data on China, as a whole, included the same five data items.

Next, the two types of data were analysed using the M-K trend test and wavelet analysis method. Finally, spatiotemporal results were displayed using ArcGIS, and sustainable drought management strategies were discussed and suggested. The research framework of this study is illustrated in Figure 2.

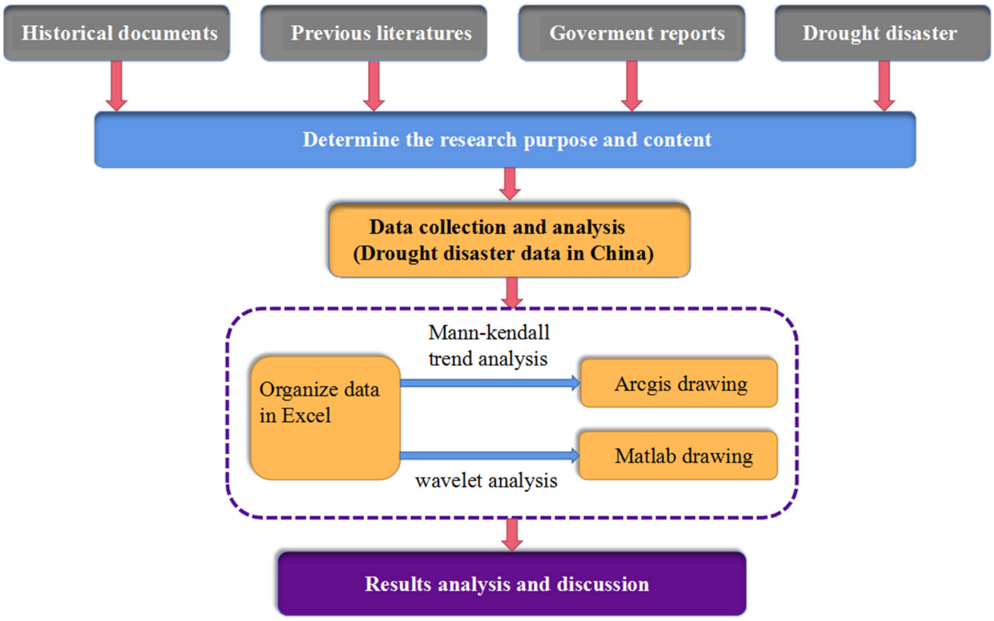

Figure 2. Research framework of this study.

2.3. Methods

2.3.1. M-K Trend Analysis

After extracting the data, the disaster data were classified and converted into an Excel database, and the trend analysis was completed using the M-K [33] trend test method, programmed in MATLAB 2011, to determine whether there was a statistically significant trend in droughts and related socioeconomic damage.

The equation of the Mann–Kendall test for trends is described as follows:

$$Z_c = \begin{cases} \frac{S-1}{\sqrt{var(S)}},\ S > 0 \\ 0, S = 0 \\ \frac{S+1}{\sqrt{var(S)}},\ S < 0 \end{cases} \quad (1)$$

$$S = \sum_{i=1}^{n-1} \sum_{k=i+1}^{n} sgn(x_k - x_i) \quad (2)$$

$$sgn(\theta) = \begin{cases} 1, \theta > 0 \\ 0, \theta = 0 \\ -1,\ \theta < 0 \end{cases} \quad (3)$$

$$var[S] = \frac{[n(n-1)(2n+5) - \sum_t t(t-1)(2t+5)]}{18} \quad (4)$$

where x_k and x_i are the data series of the economic losses, such as continuous drought disasters; n is the total length of the data set; t is the width of each unit; and $\sum$ is the sum of all units.

The indicators for the measurement of the size of the trend are:

$$\beta = Median\left(\frac{x_i - x_j}{i - j}\right), \forall j < i \quad (5)$$

In the formula, $1 < j < i < n$, where β represents the slope, a positive slope corresponds to an increase, and a negative slope to a decrease. The measurement of the value indicates that the trend is clear.

The M-K test is as follows:

Null hypothesis $H_0 : \beta = 0$.

When $|Z_c| > Z_{1-\alpha/2}$, this assumption is rejected. This indicated that the trend was significant. In the formula, $\pm Z_{1-\alpha/2}$ is the standard normal variance and α is the significance test level.

Z-tests were used to measure the statistical significance of the trends. We used this statistical test to evaluate the null hypothesis (H_0). If it is better than $Z_{\alpha/2}$, then α is chosen as the significance level (e.g., at 5%, $Z_{0.025} = 1.96$); the null hypothesis is invalid, indicating that the trend is significant.

To better represent the spatial distribution of the five drought-related disaster indicators and the related trend changes, the results were analysed using the GIS software ArcGIS, and the reasons for the changes in some provinces were discussed [34].

2.3.2. Wavelet Analysis

Wavelet analysis is a new and rapidly developing field in applied mathematics and engineering [35]. After nearly 10 years of exploration and research on wavelet analysis, an important formal system of mathematics for wavelet analysis has been established, and its theoretical foundation is more solid [36]. Compared with the Fourier transform, the wavelet transform is a local transform of space (time) and frequency; thus, it can effectively extract information from the signal. The basic idea of wavelet analysis is to use a cluster of wavelet function systems to represent or approximate a certain signal or function [37,38]. Therefore, the wavelet function is key to wavelet analysis. It refers to a function that has strong oscillation and can quickly decay to zero. That is, the wavelet function is and satisfies

$$\int_{-\infty}^{+\infty} \psi(t)dt = 0 \tag{6}$$

where $\psi(t)$ is the basis wavelet function, which is a cluster of function systems that can be obtained by the increase or decrease in the time scale and the translation on the time axis.

$$\psi a, b(t) = |a|^{-1/2}\psi\left(\frac{t-1}{2}\right), a, b \in R, a \neq 0 \tag{7}$$

where $\psi_{a,b}(t)$ is a subwavelet, α is a time scale factor, that is, the length of the wavelet period, and b is the translation factor of a translation in response time.

If it is a subwavelet according to (2), for a given energy-limited signal, $\psi(t) \in L^2(R)$, and the continuous wavelet transform (CWT) is:

$$W_f(a, b) = |a|^{-1/2} \int_R f(t)\bar{\psi}\left(\frac{t-b}{a}\right)dt \tag{8}$$

where $W_f(a, b)$is the wavelet transform coefficient, f(t) is a signal or square integrable function, a is the scaling scale, b is a translation parameter, and $\bar{\psi}\left(\frac{t-b}{a}\right)$ is the complex conjugate function of $\psi\left(\frac{t-b}{a}\right)$. The time-series data observed in this study were mostly discrete. The function $f(k\Delta t)$ is constructed (k = 1, 2, . . . , N; Δt is the sampling interval), and the discrete wavelet transform of Equation (8) is

$$W_f(a, b) = |a|^{-1/2}\Delta t \sum_{k=1}^{N} f(k\Delta t)\bar{\psi}\left(\frac{k\Delta t - b}{a}\right) \tag{9}$$

From Formulas (8) or (9), we can determine the basic principle of wavelet analysis, that is, increase or decrease the scaling scale "a" to obtain the low-frequency or high-frequency information of the signal and then analyse the overview or details of the signal to achieve different time scales and an analysis of the spatial special features [39].

In actual research, the most important task is to obtain wavelet coefficients from the wavelet transform equation and then use these coefficients to analyse the time–frequency variation characteristics of the time series.

Integrating the square value of the wavelet coefficients in the "b" domain can determine the wavelet variance:

$$Var(a) = \int_{-\infty}^{\infty} \left| W_f(a,b) \right|^2 db \tag{10}$$

The transformation process of wavelet variance with scale "a" is called the wavelet variance map. From Formula (10), it can be seen that it can reflect the distribution of the signal fluctuation energy with scale "a". Therefore, the wavelet variance map can be used to determine the relative intensity of the disturbances of different scales in the signal and the main time scale, that is, the main period.

A multiscale detailed analysis of functions or signals can be performed by computing functions such as scaling and translation, which solves many difficult problems that the Fourier transform cannot solve. Wavelet transform has connected many disciplines, such as applied mathematics, physics, computer science, signal and information processing, image processing, and seismic exploration [40]. The wavelet analysis method was used to analyse the effects of droughts, and the key factors related to droughts could be clearly compared horizontally and vertically.

3. Results

3.1. Spatial Distribution of Average Drought Disaster Data

The spatial distribution of the average drought disaster data was mainly based on the provinces, and it is expressed as the crop damage area, drought-affected area of crops, crop failure area, populations with reduced drinking water caused by drought, and domestic animals with reduced drinking water caused by drought.

In Figure 3 the results showed that the increase in drought frequency in China was mainly concentrated in the north and south. Drought was the most severe in western China; some areas in northern China were severely affected, and the situation in southern and eastern China was less severe.

In Inner Mongolia, Heilongjiang, and Liaoning, crops were affected in a dispersed area. For the rest of the provinces, the distribution was concentrated, and owing to the geographical location, it appeared at abnormal points in Heilongjiang Province. From the various boxes of the median and four-digit spans, it can be seen, from top to bottom, that, in addition to Heilongjiang, Liaoning, Jiangxi, and Qinghai provinces, the distribution was symmetrical.

In terms of crop area, some provinces in western and southeastern China were relatively less affected, and the general trend was similar to that of crops. Heilongjiang Province and Inner Mongolia have the deepest colours, indicating that they have been the hardest hit areas in recent years.

There was a close relationship between the average area affected by drought disasters and the average area of crop failure. This trend was similar in the affected areas.

The average number of people and livestock with reduced drinking water owing to drought was the most dispersed in Inner Mongolia, Sichuan, and Yunnan provinces, indicating that the average number of livestock with reduced drinking water owing to drought was the largest in these three provinces, and the trend was similar in the affected areas. Inner Mongolia, Heilongjiang, Yunnan, Sichuan, and Guizhou provinces experienced economic losses caused by drought.

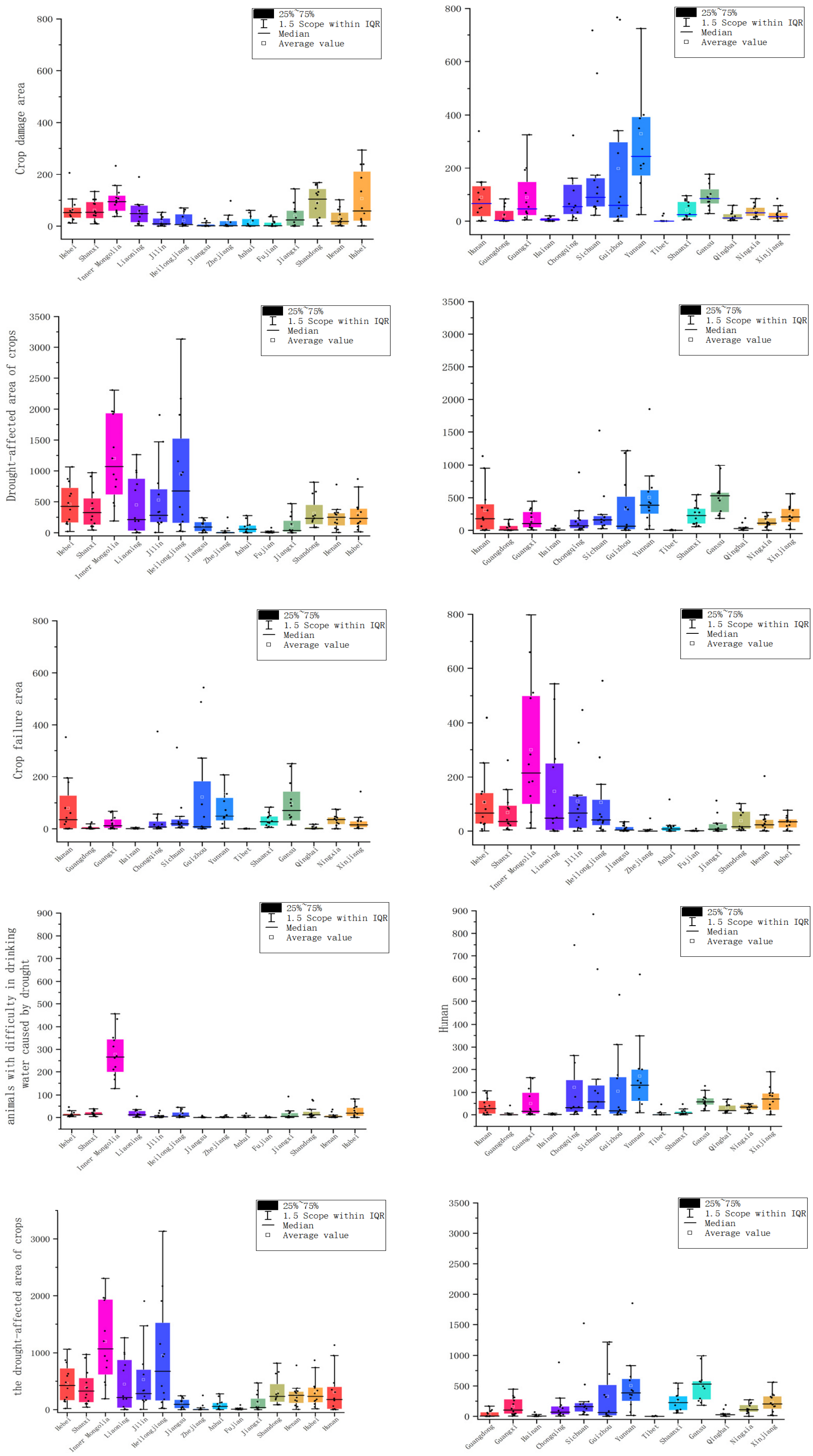

Figure 3. Drought distribution map of the provinces over the last 20 years.

In Figure 4a,b, the average drought data for each province in China are shown, with six different colours indicating different grades. The darkest colour indicates the most severe level of drought and the lightest colour indicates the lightest level of drought.

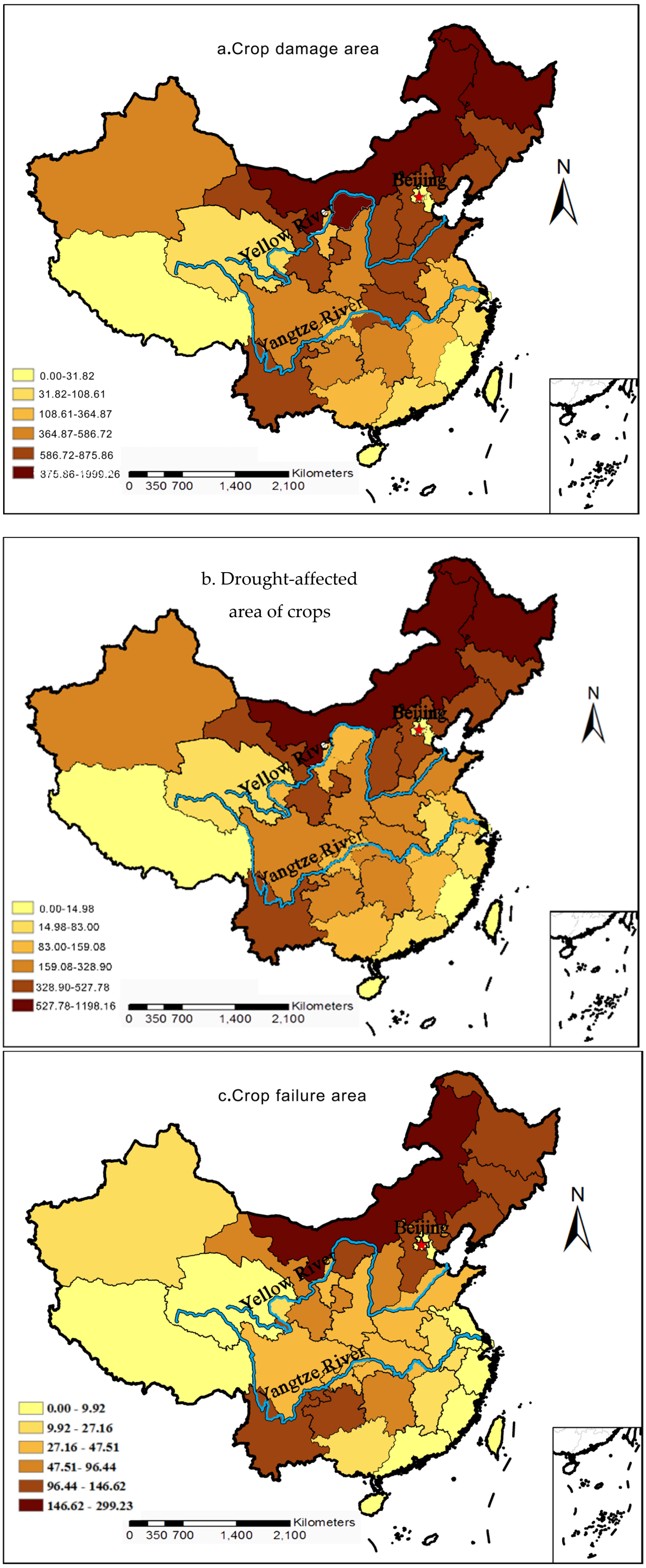

Figure 4. *Cont.*

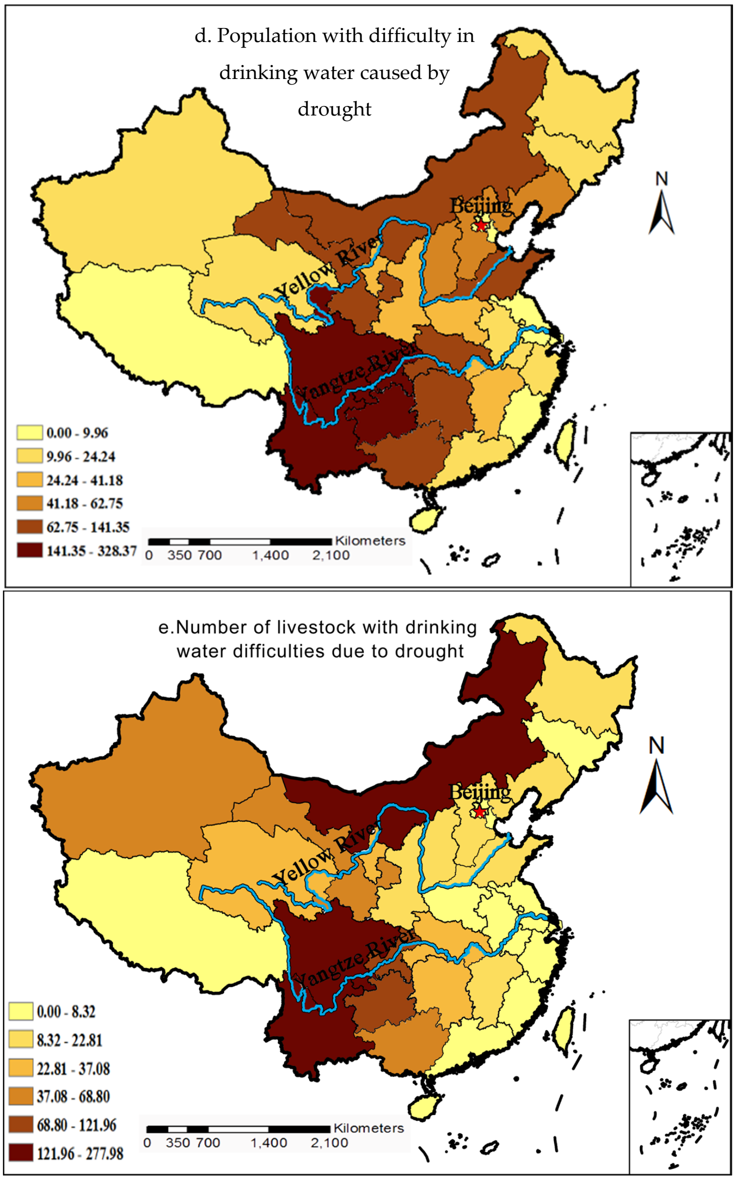

Figure 4. National average provincial drought disaster conditions.

3.1.1. Crop Damage Area

A crop-damaged area is an area suffering from drought that has reduced crop production by more than 10% from the normal annual yield. The same cropland affected in multiple seasons was counted only once. From the perspective of the average crop area affected by a drought disaster, as shown in Figure 4a, the darkest grade was 875.86–1999.26 $\times$ 10^3 ha, which represents the province with the highest average crop area affected by drought disasters. Some provinces in north China, northeast China, central China, Yunnan, and other provinces had large disaster areas, whereas some provinces in western China and southeast China had relatively few disaster areas [41]. The two provinces (autonomous regions) of Heilongjiang and Inner Mongolia had the darkest colours, indicating that they had the most crop-stricken areas. The average crop area affected by drought disasters in Heilongjiang Province has reached 1843.609 $\times$ 10^3 ha in recent years, and the average crop area affected by drought disasters in Inner Mongolia reached 1999.262 $\times$ 10^3 ha. The impact of such disasters on crop damage areas was prominently reflected in 2007 and 2009.

In 2007, drought disasters in China were serious [42]. The crop damage area in the country was 29,386 × 10^3 ha, which was prominently reflected in Heilongjiang Province. The crop damage area in Heilongjiang Province was 6500 × 10^3 ha. Traditional rainy, flood-prone, and the main grain-producing areas were heavily affected by drought [43]. In 2007, droughts lasted for one month in parts of Jiangnan and South China, with abundant annual rainfall in 2007 and over 40 days in severely drought-prone areas. Some areas have experienced early autumn and winter. More serious droughts and disasters have occurred in northeast China and in the middle and lower reaches of the Yangtze River, an important commercial grain base in China, and the second most severe drought has occurred in the northeast Sanjiang (Heilongjiang, Ussuri, and Songhua rivers) Plain since 1949 [44]. The Sanjiang Plain is crucial for ensuring food security in Heilongjiang Province and the whole country. However, since 2000, droughts have occurred frequently in the Sanjiang Plain as an unconventional early zone [45], and the situation has intensified. Droughts of varying degrees occur each year. More serious droughts and disasters have occurred in northeast China and in the middle and lower reaches of the Yangtze River, an important commercial grain base in China. In most areas, there was no effective rainfall for more than 40 days. At the same time, reservoirs dried up, and rivers were cut off, which had serious impacts on industrial and agricultural production. Owing to the occurrence of droughts, Heilongjiang, Inner Mongolia, Jilin, Hunan, Liaoning, Hebei, Shanxi, Shandong, Jiangxi, and another nine provinces experienced huge losses of food, amounting to 27.93 billion kg and 75% of total national food losses owing to drought, and Heilongjiang, Inner Mongolia, and Jilin accounted for a large proportion. The annual loss owing to drought disasters in the country was relatively large, and the annual average was high. The crop damage, drought-affected, and crop failure areas across the country were significantly greater than the average from 1991 to 2006. The country's early grain losses rank fifth since 1991, reaching 37.36 billion kg, which is 8.95 billion kg more than the average in 1991–2006.

In 2009, China's drought disaster was relatively severe. This was a year of severe drought. The crop damage area was significantly larger than the average of 25,133.82 × 10^3 ha from 1991 to 2008. The drought disaster was prominent in Inner Mongolia, where the crop-affected area was 3890.1 × 10^3 ha. In May 2009, during the spring drought in northwestern northeast China, during the peak drought period, the drought area of cultivated land in Inner Mongolia was 2545 × 10^3 ha, and the area of dry grasslands in pastoral areas was 460,000 km^2, accounting for more than two-thirds of the available grasslands in the region. Among these, drought was the most serious in the main grain production areas of the East Four League. From late July to mid-August, summer drought occurred in the western part of northeast China, and the average rainfall was generally 50% to 90% lower during the same period of the year. The drought situation in Inner Mongolia, eastern and southern China, and other regions rapidly spread and developed. In mid-August, four provinces, including Liaoning, Jilin, Inner Mongolia, and Heilongjiang, suffered a drought area of 9600 hectares, accounting for approximately 75.31% of the national drought area during the same period.

3.1.2. The Drought-Affected Area of Crops

The drought-affected area refers to the area where the crop output is reduced by more than or equal to 30% from the normal annual output owing to drought. From the perspective of the average crop disaster area shown in Figure 4b, the darkest grade was 527.78–1198.16 × 10^3 ha, which represents the province with the largest area in terms of the average drought-affected area of crops. Some provinces in northern China, northeast China, central China, Yunnan, and other provinces had large disaster areas, whereas some provinces in western and southeast China had relatively few disaster areas, and the overall trend was similar to that of crops [46]. Heilongjiang Province and Inner Mongolia had the darkest colours, indicating that these areas were most affected by disasters in recent years. This is consistent with the average crop area affected by drought disasters, as shown in Figure 4a. The difference is that the average crop disaster areas in the three provinces of

Shandong, Henan, and Hubei were at the third level, which was better than the average crop area affected by drought disasters. In recent years, the average crop disaster area in Heilongjiang Province reached 944.538 $\times$ 10^3 ha, and the average crop disaster area in Inner Mongolia reached 119.8160 $\times$ 10^3 ha. The impact of drought disasters on crop disaster areas was also prominent in 2007 and 2009.

In 2007, China's drought disaster had a significant impact on crops. The country had 16,170.00 $\times$ 10^3 ha of drought-affected crop areas, and the direct economic loss from drought disasters was CNY 109.37 billion. In August, severe drought occurred in Heilongjiang, western Jilin, eastern Inner Mongolia, Jiangxi, southwestern Hunan, and northwestern Guangxi, which had a significant impact. The drought area of cultivated land nationwide reached 115.33 million hectares. This was particularly serious in Heilongjiang Province. Several rivers had the lowest water level during the same period in history, and the phenomena of dried-out reservoirs and insufficient water output from electromechanical wells were frequent. The crops were heavily affected by drought, with an area of 6467 $\times$ 10^3 ha, accounting for 55% of the sown area.

In 2009, China's drought disaster also had a greater impact on the drought-affected area of crops, with 13,197.10 $\times$ 10^3 ha owing to nationwide drought The area affected by drought crops was equivalent to the average area since 1991. The loss from drought disasters was relatively high on an average annual basis. The staged drought conditions were outstanding and had a long duration and a wide range of droughts, which had a significant impact on the area of crop disasters.

3.1.3. Crop Failure Area

The crop failure area refers to the area in which the crop yield was reduced by more than or equal to 80% from the normal annual output because of early drying. From the perspective of the average total crop failure area shown in Figure 4c, the darkest grade was 146.62–299.23 $\times$ 10^3 ha. This level represents the province with the largest total crop failure area. Some provinces in northern and northeastern China and Yunnan and other provinces had a large total crop failure area, whereas some provinces in western, eastern, and southeastern China had relatively small crop areas. Inner Mongolia had the darkest grade, indicating that Inner Mongolia had the largest average total crop failure area in recent years. Inner Mongolia achieved an average crop failure area of 299.228 $\times$ 10^3 ha. In Heilongjiang, Jilin, Liaoning, Hebei, Yunnan, and Guizhou, large crop failure areas occurred in recent years, and the average total crop failure areas were 106.569, 111.113, 146.620, 107.151, 134.238, and 121.778 $\times$ 10^3 ha, respectively. The impact of drought disasters on crop failure areas was prominently reflected in 2007. The drought disaster in China had a significant impact on the crop failure area, with 3190.67 $\times$ 10^3 ha. In 2009, drought disasters also had a significant impact on the crop failure area, with 3268.80 $\times$ 10^3 ha.

As shown in Figure 4a–c, the relationship between the average crop area affected by drought disasters, the average drought-affected area of crops, and the average crop failure area was relatively close, and the trends in the affected areas were also similar. Comparing Figure 4a–c, it can also be seen that the agricultural drought disaster in Inner Mongolia was the most serious, and the average crop area affected by the drought disaster, the average drought-affected area of crops, and the average crop failure area were also the largest. In Inner Mongolia, precipitation has decreased in recent years and the climate is characterised by warming and drying. Crop drought disasters are affected by temperature and precipitation.

3.1.4. People and Livestock with Reduced Drinking Water Owing to Drought

The average number of people and domestic animals with reduced drinking water caused by drought is shown in Figure 4d,e, which were mainly highlighted in Yunnan, Sichuan, Chongqing, Inner Mongolia, and other provinces (autonomous regions and municipalities). As can be seen from Figure 4d, the darkest level was 141.35–328.37 (ten thousand people), and this level represents the provinces with the largest number of people with reduced drinking water caused by drought. The three provinces of Yunnan, Sichuan, and Guizhou had the darkest colours, indicating that these three provinces had the largest average number of people reduced drinking water caused by drought, at 328.368, 178.069, and 197.963 million, respectively. As can be seen from Figure 4e, the darkest level was 121.96–277.98 (ten thousand people), which represents the province with the largest average number of domestic animals with reduced drinking water caused by drought. The three provinces of Inner Mongolia, Sichuan, and Yunnan had the darkest colours, indicating that these three provinces had the largest average number of domestic animals with reduced drinking water caused by drought, with 277.978, 174.584, and 1.7734 million, respectively. As shown in Figure 4d, the average number of people with reduced drinking water in Inner Mongolia caused by drought was second, but in Figure 4e. The average number of domestic animals was the first level. The average number of domestic animals with reduced drinking water caused by drought in Inner Mongolia was much larger than the average number of people with reduced drinking water caused by drought.

In Yunnan Province, the number of people and domestic animals with reduced drinking water caused by drought was prominently reflected in 2010. The main reason for this is that from autumn 2009 to the beginning of April 2010, the precipitation in Yunnan decreased more than that in the same period of many years, approaching or breaking the historical extreme value, resulting in a serious dry flow of hundreds of small- and medium-sized rivers and the drying of reservoirs. The water storage capacity was significantly reduced. Owing to the low precipitation and inflow of the river, drought in Yunnan Province began to appear and spread rapidly in November. By February 2010, the drought had intensified. At the beginning of April, when the drought was the most severe, the drought area of cultivated land in the five southwestern provinces was relatively large, making it difficult for tens of millions of people and domestic animals to obtain drinking water. Some places have reached extreme drought levels.

In Sichuan Province and Chongqing, the number of people and domestic animals with drinking water caused by drought was prominently reflected in 2006. The main reason is that there was a rare summer drought in eastern Sichuan during this period, and a major drought occurred in Chongqing and eastern Sichuan. The drought lasted for a long time and had high intensity. The loss was extremely serious, and it was the most serious since the data began to be recorded in 1891. In July, the average temperature in Sichuan, Chongqing, and other places reached its highest level in the same period since 1951. Affected by factors such as high temperature and low rainfall, drought occurred in many places and continued to develop. In August, the temperature continued to increase and drought continued to develop.

In Inner Mongolia, the number of people and domestic animals with reduced drinking water owing to drought was prominently reflected in 2009. Throughout the year, 17.5600 million rural people and 10.9400 million large domestic animals had reduced drinking water owing to drought. Eighty-nine cities suffered from water shortages of varying degrees, affecting 16.6698 million urban residents. In May, the drought in Inner Mongolia was severe. There were 820,000 people and 2.07 million large domestic animals with reduced drinking water owing to drought. Herdsmen must obtain water up to a distance of 20 km. In August, the northwestern part of the country suffered from droughts in the summer owing to reduced drinking water.

3.2. Result of Z-Value

3.2.1. Z-Value Overall Analysis

In Figure 5 each row in the heat map represents a province, and each column is an indicator; a darker colour indicates that the M-K trend test did not pass, and a lighter colour indicates that the M-K trend test passed at the significance level. By analysing the heat map, it is clear that the provinces (districts and cities) of Gansu, Sichuan, Shaanxi, Hebei, Beijing, Guangxi, Guangdong, Hainan, and Zhejiang passed the M-K trend test, the crop area affected by drought in these provinces was significantly reduced, and the situation was effectively controlled. The replicability of all five samples was good, proving that the derived data were credible, reliable, and logical. It also visually demonstrates the variation in the expression data of the study subjects, which was not large for almost every province, except Inner Mongolia, which is an idiosyncratic point: Inner Mongolia passed the M-K trend test and reached a significant level for the number of livestock with reduced drinking water owing to drought, showing a significant upward trend. The remaining provinces passed the M-K test.

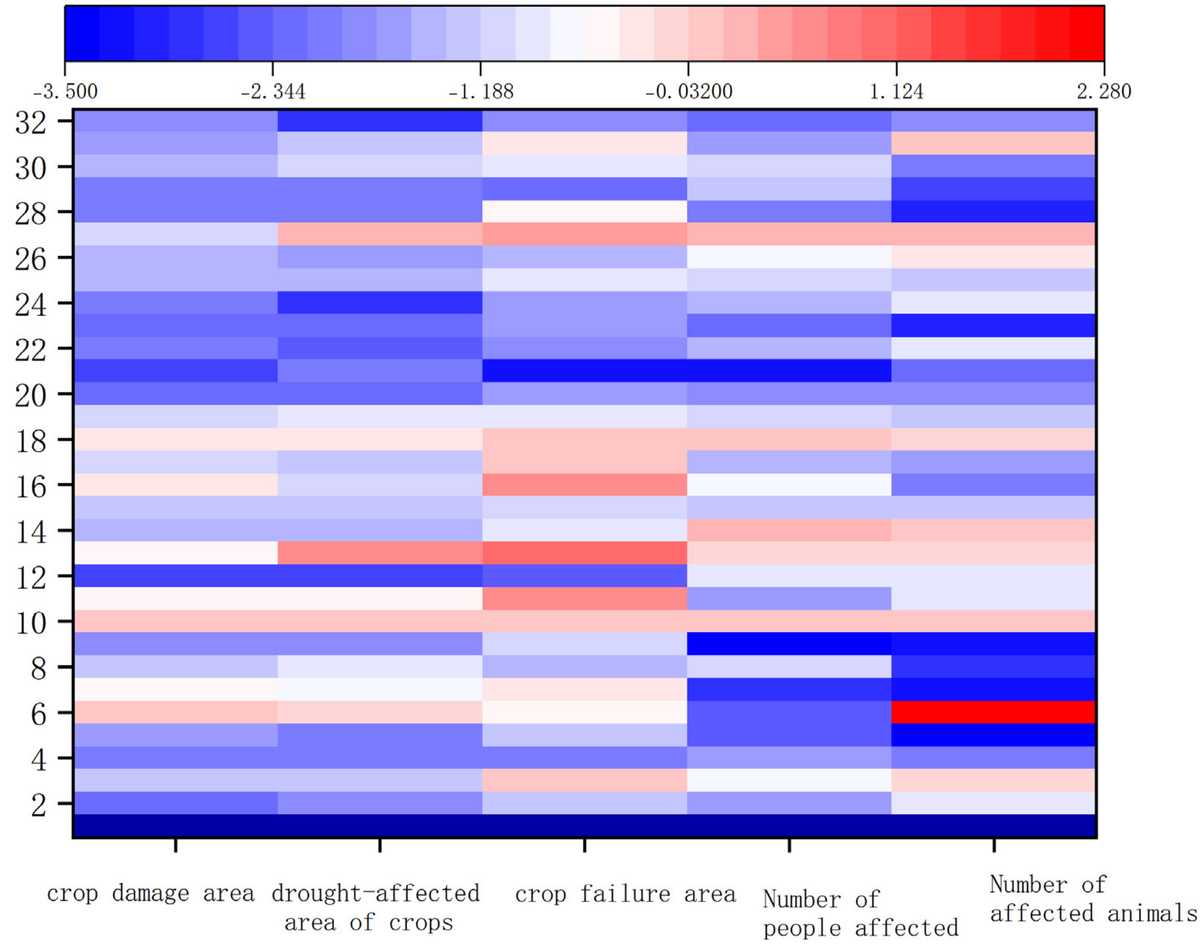

Figure 5. Heat map of the variation of drought indicators (1—blank control; 2—Beijing; 3—Tianjin; 4—Hebei; 5—Shanxi; 6—Inner Mongolia; 7—Liaoning; 8—Jilin; 9—Heilongjiang; 10—Shanghai; 11—Jiangsu; 12—Zhejiang; 13—Anhui; 14—Fujian; 15—Jiangxi; 16—Shandong; 17—Henan; 18—Hubei; 19—Hunan; 20—Guangdong; 21—Guangxi; 22—Hainan; 23—Chongqing; 24—Sichuan; 25—Guizhou; 26—Yunnan; 27—Tibet; 28—Shaanxi; 29—Gansu; 30—Qinghai; 31—Ningxia; 32—Xinjiang).

3.2.2. Z-Value Space Analysis

In the analysis of the crop disaster area, as shown in Figure 6a, the crop damage areas all showed a decreasing trend nationwide, but only Gansu, Sichuan, Shaanxi, Hebei, Beijing, Guangxi, Guangdong, Hainan, and Zhejiang provinces (autonomous regions and municipalities) passed the M-K test. The trend test reached a significant level, with Z-values of −1.9886, −2.1257, −2.1257, −1.9886, −2.3315, −2.66743, −2.2629, −2.1257, and −2.6743, respectively. This shows that the crop areas affected by drought disasters in these provinces were significantly reduced and the situations were effectively controlled. The value of the M-K trend Z-value in the other provinces was lower than −1.96, indicating that the change trend was not significant. As can be seen from the graph, the area affected by crops nationwide was on a downward trend, which showed that China has made unremitting efforts in recent years to combat drought and achieved certain results. In recent years, China has formed a pattern of optimising the allocation of water resources in the form of "four horizontal and three vertical north–south deployments and east–west mutual assistance", as per the Regulations of the People's Republic of China on Drought Control, promulgated and implemented in 2009. It has also made drought control work rule- and law-based. China has also established a national drought monitoring and forecasting and drought control command and decision support system, and the level of drought monitoring capability, drought control command capability, decision-making modernisation, and information technology have improved. The development of the national drought emergency response capacity has been steadily promoted, and the preparation of drought prevention plans at the provincial, municipal, and county levels has been completed, forming a more comprehensive drought prevention plan system. Drought preparedness plans at the county level were developed at the national level. A socialised drought service network based on service teams, township drought service teams, village drought teams, and farmers' drought associations has played an important role in emergency drought relief during major droughts. At the same time, China has also increased the capacity of the vegetation to contain water by planting trees, building reservoirs, and implementing inter-basin water transfer projects to solve water shortages during the irrigation season and in water-scarce areas, developed water-saving agriculture in drier areas by planting drought-tolerant crops, developing water-saving irrigation, protecting wetlands and vegetation, and taking other measures to cope with drought. With the gradual establishment of China's meteorological disaster system, awareness of crop disaster prevention in China has gradually increased, reducing the area affected by China's crops and lowering farmers' economic losses.

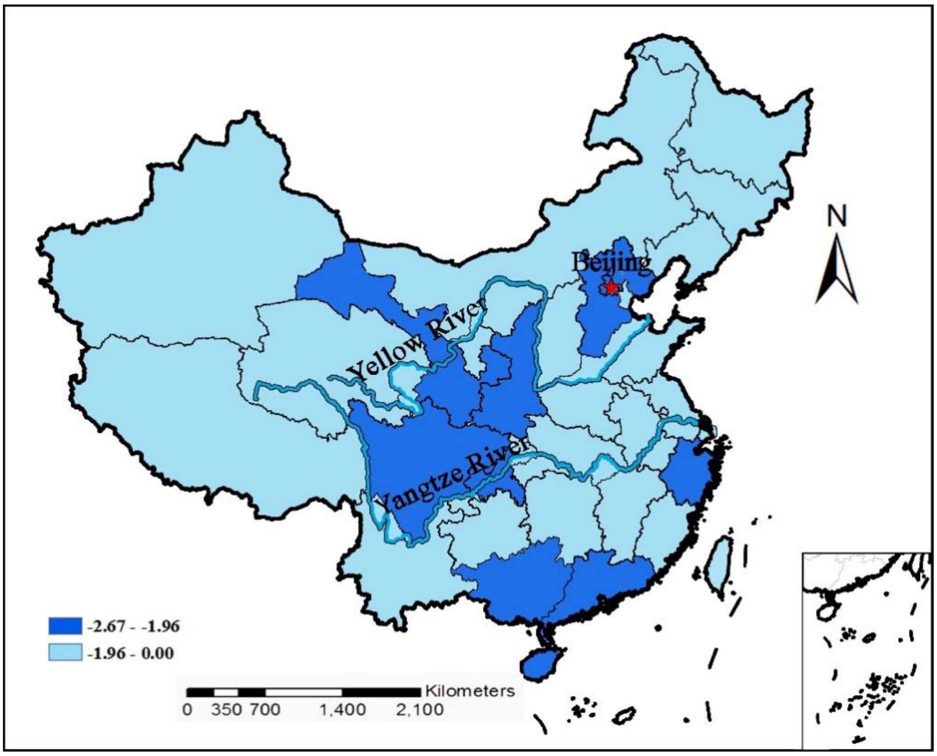

(**a**)

Figure 6. *Cont.*

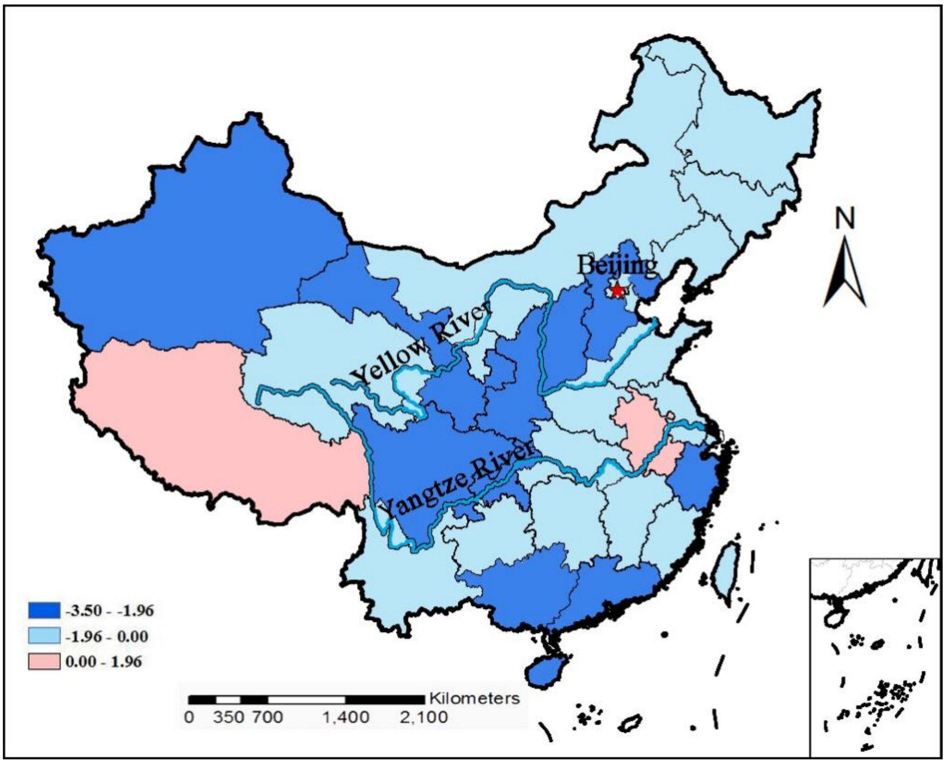

(**b**)

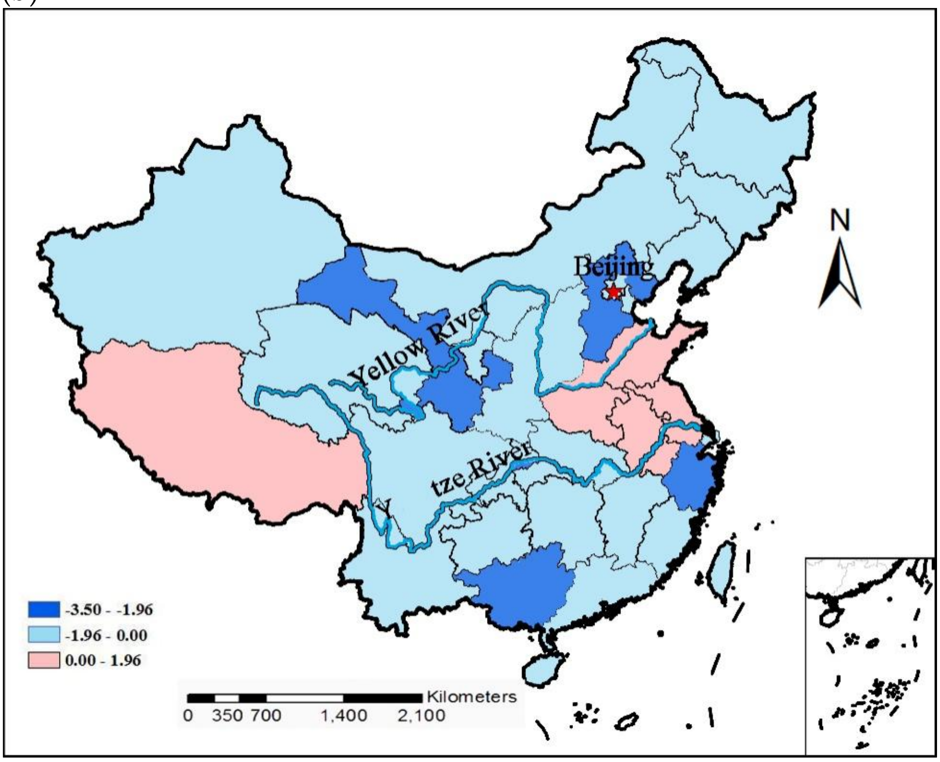

(**c**)

Figure 6. *Cont.*

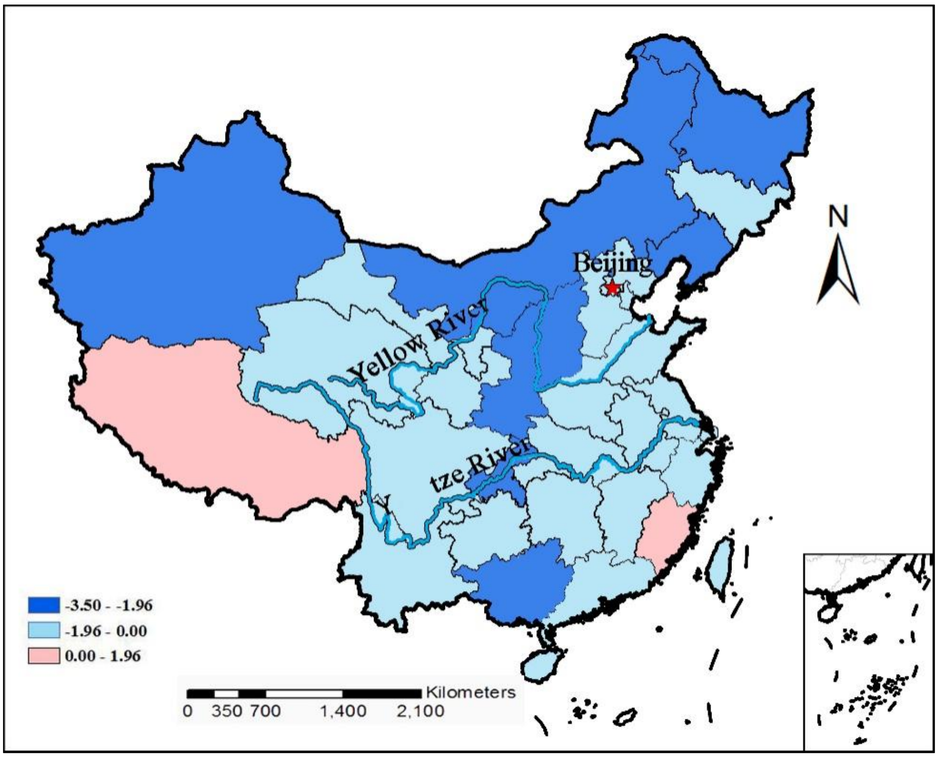

(**d**)

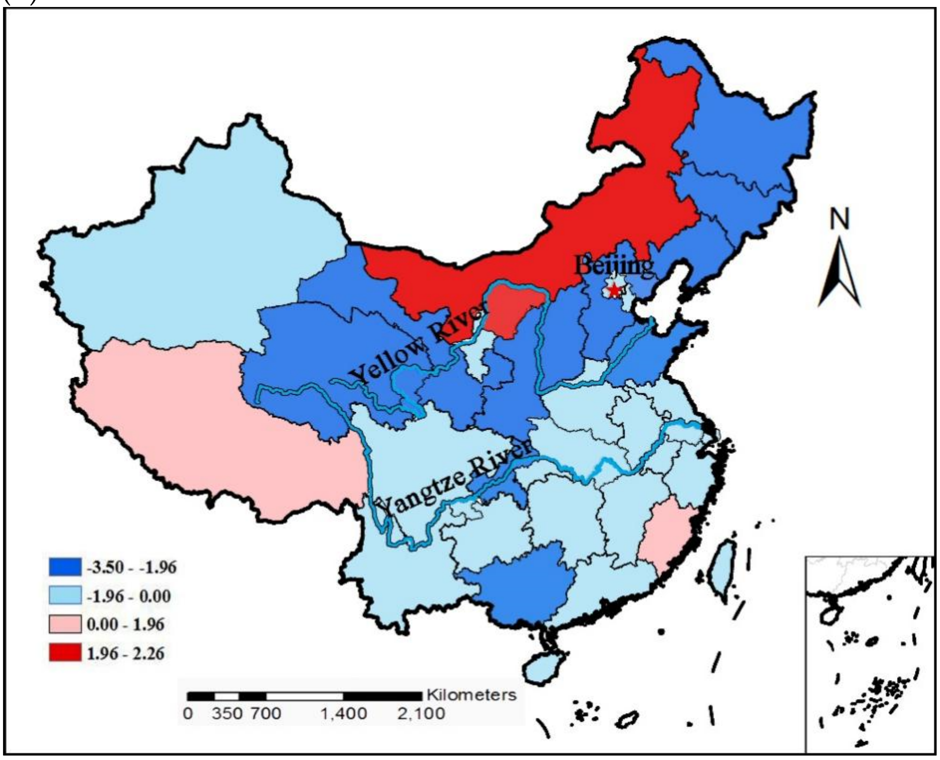

(**e**)

Figure 6. Z-value of the national disaster data over the past 12 years: (**a**) crop damage area; (**b**) crop area with drought disaster; (**c**) total crop failure area; (**d**) number of people with reduced drinking water owing to drought; (**e**) number of domestic animals with reduced drinking water caused by drought.

From the analysis of the drought-affected area of crops, which can be seen in Figure 6b, although Tibet and Anhui provinces showed increasing trends, with Z-values of 0.34286 and 0.68573, respectively, neither province passed the M-K trend test, indicating that the change trends were not significant. The remaining provinces show a decreasing trend. Xinjiang, Gansu, Sichuan, Shaanxi, Shanxi, Hebei, Zhejiang, Guangxi, Guangdong, and Hainan provinces reached significant levels through the M-K trend test, indicating that the crop disaster area was significantly reduced and effectively controlled. The Z-values were −2.8115, −2.1257, −2.8115, −2.1257, −1.9886, −1.9886, −2.6743, −2.1257, −2.2629, and −2.4000, respectively. No other province passed the M-K trend test, indicating that the change trends were not significant. This shows that the crop disaster area decreased, but not significantly.

From the analysis of the crop failure area, as shown in Figure 6c, it can be seen that the provinces of Tibet, Anhui, Shandong, Jiangsu, and Henan showed an upward trend, but none of them passed the M-K trend test, indicating an insignificant change trend. The remaining provinces show a decreasing trend. Among them, Gansu, Hebei, Guangxi, and Hainan passed the M-K trend test, reaching a significant level, with Z-values of −2.2629, −2.1257, −3.2229, and −1.8515, respectively, in increasing order. This indicated that the area of crop failure was significantly reduced and effectively controlled. No other province passed the M-K trend test, indicating an insignificant change trend, suggesting that the crop area was reduced again but not significantly.

The number of people and livestock with reduced drinking water owing to drought were analysed together. From the analysis in Figure 6d, it can be seen that Tibet and Fujian provinces showed an upward trend, but neither of them passed the M-K trend test, indicating that the change trend was not very obvious. The number of people with reduced drinking water owing to drought in these two provinces increased but not significantly. The remaining provinces show a decreasing trend. Xinjiang, Inner Mongolia, Heilongjiang, Liaoning, Shaanxi, Shanxi, Chongqing, and Guangxi passed the M-K trend test to reach a significant level, with Z-values of −2.2629, −2.4, −3.3601, −2.8115, −1.9886, −2.4686, −2.2629, and −3.2229, respectively. This indicates that the number of people and livestock with reduced drinking water was significantly decreased and effectively controlled. No other province passed the M-K trend test, indicating an insignificant change trend, suggesting that the number of people with reduced drinking water owing to drought decreased, but not significantly.

Figure 6e shows that the number of livestock in the provinces of Inner Mongolia, Tibet, and Fujian is increasing. Inner Mongolia passed the M-K trend test with a Z-value of 2.2629, indicating a clear change trend and a significant increase in the number of livestock reduced drinking water caused by drought. Tibet and Fujian provinces did not pass the M-K trend test, indicating that the trend was not significant. This suggests that the number of livestock with reduced drinking water owing to drought increased in these two provinces, but not significantly. The data from the remaining provinces showed a decreasing trend. Among them, Heilongjiang, Jilin, Liaoning, Hebei, Shandong, Shanxi, Shaanxi, Gansu, Qinghai [47], Chongqing, and Guangxi reached a significant level in the M-K trend test with Z-values of −3.2229, −2.88, −3.2229, −2.1257, −2.1257, −3.4972, −3.0858, −2.66743, −1.9886, −3.0858, and −2.2629, respectively. This indicates that the number of people with reduced drinking water owing to drought has been significantly reduced and effectively controlled.

In Inner Mongolia, there has been a marked increase in drought-induced water difficulties for livestock. This impact was more severe in 2016 and 2010. Inner Mongolia is a region in China with severe water shortages. The droughts are mainly located in the southwestern part of Erdos City, northwestern part of Hulunbeier City, Baotou City, and Xilin Gol League. The total water resources in the region are relatively small at 50.885 million cubic meter, accounting for approximately 5.1% of the country's total water resources. The region's annual per capita water consumption is lower than the national average, with over 600 cubic meters of water used per hectare of land, which is equivalent to one-fifth of the national average. This, coupled with the uneven distribution of water resources in time and space, has caused natural disasters of varying degrees throughout the region every year, particularly sandstorms and droughts. In recent years, the number of droughts in Inner Mongolia has increased significantly, particularly from 2015 to 2017. Drought has increased the area of drought-affected farmland across the region. A total of 500 million mu of pastureland has been affected, nearly 50% of which has not turned green, causing difficulties in drinking water for thousands of livestock. Approximately 300,000 livestock heads died as a result of the disaster, with direct economic losses of up to CNY 80 million. The current situation of the water resources in the region shows that there is a shortage of water, on the one hand, and the rational development and use of water resources, on the other. Scientifically carrying out the protection and construction, development, and utilisation of water resources and solving the contradiction between supply and demand of water resources has also become an important issue faced by Inner Mongolia in implementing a western development strategy. At present, Inner Mongolia has formulated plans for the protection, development, and utilisation of water resources in different river basins, according to the current situation of water resources in the region. Among them, the management of large rivers and streams, urban and rural water supply projects, water-saving irrigation of farmland and grass pastures, and the construction of soil and water conservation features prominently in the plans, especially the content of water-saving irrigation. As of 10 July 2019 200,000 people have been involved in drought relief in Inner Mongolia, more than 70,000 electric wells and 58 pumping stations have been opened, more than CNY 20 million in drought relief funds have been raised from drought areas, and drought relief repair and rehabilitation services have been organised. A total of 3000 sets of various drought relief facilities were repaired for drought relief water supply projects. Chongqing and Guangxi reached a significant level through the M-K trend test, and their Z-values were −3.2229, −2.88, −3.2229, −2.1257, −2.1257, −3.4972, −3.0858, −2.66743, −1.9886, −3.0858, and −2.2629, respectively. This shows that the number of people with reduced drinking water owing to drought was significantly decreased and effectively controlled.

3.3. Wavelet Analysis

3.3.1. Crop Damage Area

By analysing the wavelet variance map of the crop damage area in the country from 1991 to 2018 (see Figure 7), we can see that there were two more obvious peaks in the wavelet variance, which corresponded to the time change periods of 8 and 50 years. Among them, the 50 year cycle had the largest variance value, which can be judged to be the strongest over a period of approximately 50 years. This is the first main cycle of the annual change when the crop area is affected by drought disasters in the country, and the 8 year time scale was the second main cycle.

Through an analysis of the contour map of the real part of the wavelet coefficients of the crop damage area of the country from 1991 to 2018, the abscissa is the time (years), the ordinate is the time scale, and the iso-curve in the figure is the real value of the wavelet coefficient. The contour map of the real part of the wavelet coefficient reflects the periodic changes in the crop damage area at different time scales and their distribution in the time domain. It can then predict the future trend of the crop damage area at different timescales. The figure clearly shows the fluctuation of the real part of the wavelet transform coefficients, which is specifically reflected in the characteristics of alternating the crop damage area of the country to a greater or lesser extent. The conclusions are as follows.

Fluctuations in the scales at approximately 8a and 50a were obvious, and the positive and negative phases appeared alternately. Evidently, the fluctuations in the crop damage area were more and less in the calculation time domain. During the evolution of the crop damage area in China from 1991 to 2018, there were 33 to 50 year and 2 to 12 year change cycles. Among them, the quasi-two shocks that alternated over a period of 33 to 50 years were in 2002 and 2018, respectively. There were six quasi-shocks in the 2–12 year cycle, but the shocks were generally weak. Over the entire time scale, there was one more centre and one less centre in 2002 and 2018, respectively. At the 33–50 year time scale, there was obviously one more centre and one less centre in 2002 and 2018, respectively; at the 2–12 year time scale, there were six periodic oscillation centres. Additionally, there were three more centres and three fewer centres, namely, in 1993, 2001, 2008, and 1997, and 2005 and 2013, but they were all weak.

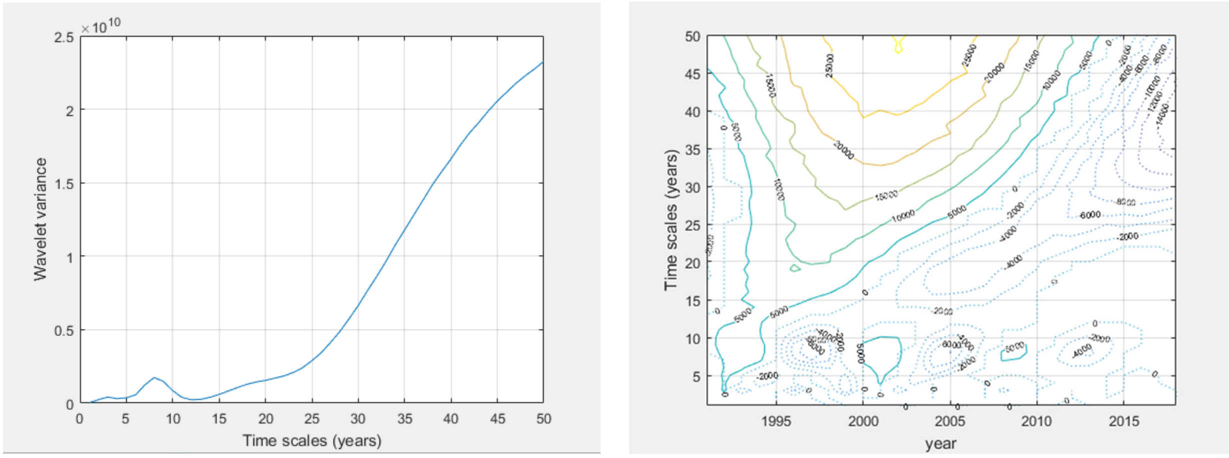

Figure 7. Wavelet square difference map and the real part of the contour map of the crop disaster area from 1991 to 2018.

3.3.2. Drought-Affected Area of Crops

By analysing the wavelet variance map of the crop disaster area in the country from 1991 to 2018 (see Figure 8), it can be seen that there were three more obvious peaks in the wavelet variance, corresponding to time changes of 3, 8, and 50 years. Among them, the 50 year cycle had the largest variance value, which was strongest in the period of approximately 50 years. This was the first main cycle of the annual change in the crop disaster area in the country, the 8 year time scale was the second main cycle, and the 3 year time scale was the third main cycle.

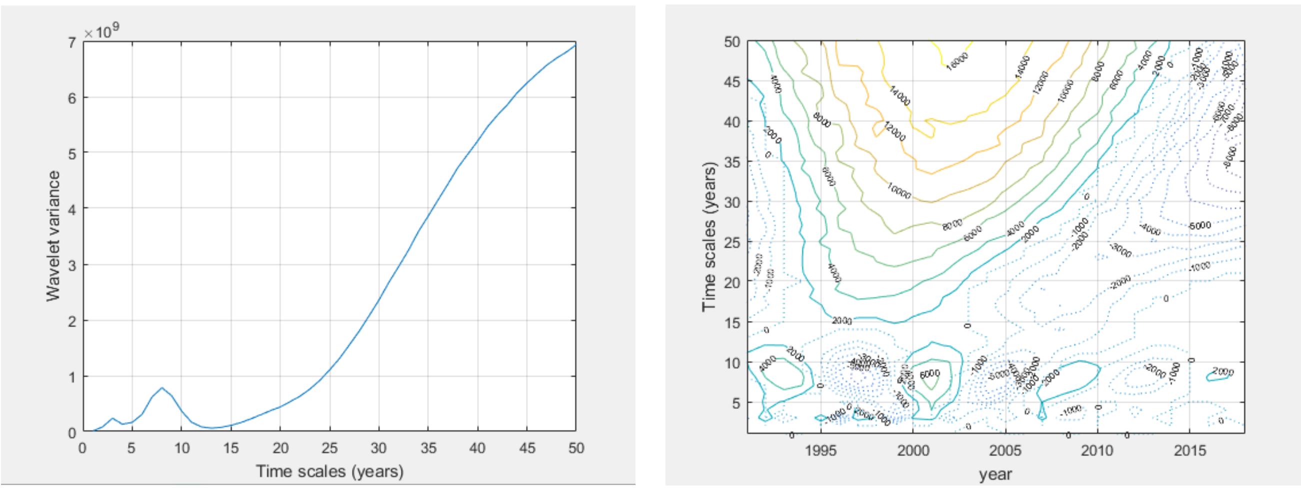

Figure 8. Wavelet square difference map and the real part contour map of the wavelet coefficients of the crop drought-affected area from 1991 to 2018.

The analysis of the contour map of the real part of the wavelet coefficients of the crop disaster area in the country from 1991 to 2018 clearly shows the fluctuation characteristics of the real part of the wavelet transform coefficients, which is specifically reflected in the characteristics of alternating crop disaster areas across the country. It can be seen that the fluctuations at scales of approximately 8a and 50a are very obvious, and the positive and negative phases appear alternately. The fluctuations in the crop disaster area were more and less in the calculation time domain. During the evolution of crop disaster areas in China from 1991 to 2018, there were 33–50 years and 2–12 years of change cycles. Among them, the number of quasi-two shocks that alternated over a period of 33 to 50 years was in 2002 and 2018, respectively. There were seven quasi-shocks in the 2–12 year cycle, but the shocks were generally weak. Over the entire time scale, there was one more centre and one less centre in 2002 and 2018, respectively. At the 33–50 year time scale, there was one more centre and one less centre, respectively, in 2002 and 2018; at the 2–12 year time scale, there were seven periodic oscillation centres, and among them there were four more centres and three less centres, namely, in 1993, 2001, 2008, 2017, and 1997, and 2005 and 2013, but they were all weak.

3.3.3. Crop Failure Area

By analysing the wavelet variance map of the national crop failure area from 1991 to 2018 (see Figure 9), it can be seen that there were two more obvious peaks in the wavelet variance, which corresponded to the time change periods of 8 and 50 years. Among them, the variance value of the 50 year cycle was the largest, and the cycle fluctuation of approximately 50 years was the strongest, which was the first main cycle of the annual change in the crop failure area in the country, and the 8 year time scale was the second main cycle.

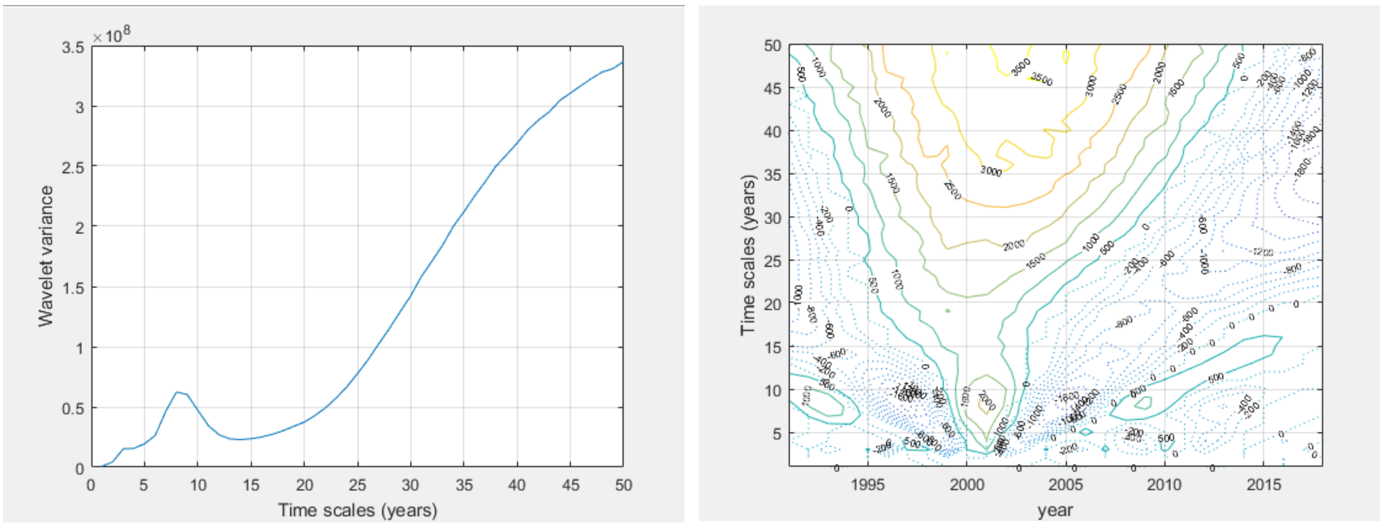

Figure 9. Wavelet square difference plot and the real part contour plot of the wavelet coefficients of the national crop failure area from 1991 to 2018.

By analysing the contour plot of the real part of the wavelet coefficients of the national crop failure area from 1991 to 2018, the graph clearly shows the fluctuation characteristics of the real part of the wavelet transform coefficients, which are specifically reflected in the characteristics of the crop failure area in the country. The conclusions are as follows:

Fluctuations at scales of approximately 8a and 50a were obvious, and the positive and negative phases appeared alternately. Evidently, the fluctuations in the crop failure area were more and less in the calculation time domain. During the evolution of the crop failure area in China from 1991 to 2018, there were 32 50 year and 4 12 year change cycles. Among them, the number of quasi-two shocks that alternated over a period of 32–50 years was in 2002 and 2018. There were five quasi-shocks in the 4–12 year cycle, but the shocks were generally weak. Over the entire time scale, there was one more centre and one less centre in 2002 and 2018, respectively. At the 33–50 year time scale, there was one more obvious centre and one less obvious centre in 2002 and 2018, respectively; at the 4–12 year time scale, there were five periodic oscillation centres. There were three more centres and two fewer centres in 1992, 2001, 2009, 1997, and 2005, but they were all weak.

3.3.4. People with Reduced Drinking Water Caused by Drought

By analysing the wavelet variance chart of the number of people with reduced drinking water owing to drought from 1991 to 2018 (see Figure 10), we can see that there were three more obvious peaks in the wavelet variance, corresponding to 10-, 17, and 50 year time change cycles. Among them, the 50 year cycle had the largest variance value, which was the strongest in the period of approximately 50 years. This was the first main cycle of the annual change in the crop damage area in the country, the 17 year time scale was the second main cycle, and the 10 year time scale was the third main cycle.

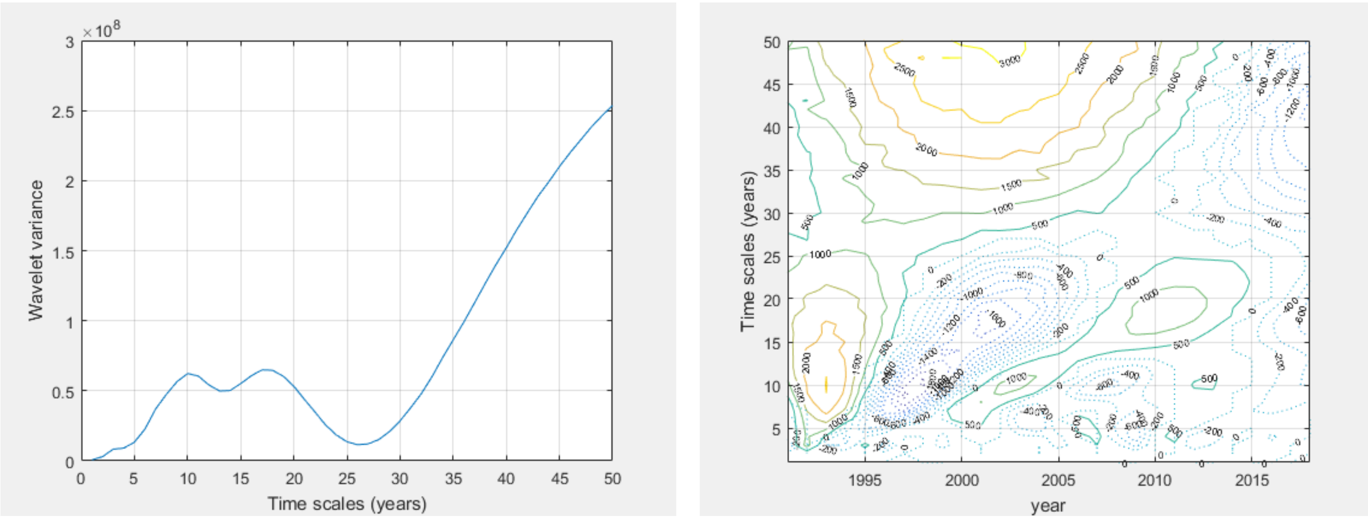

Figure 10. Wavelet variogram and coefficient real part contour plot of the number of people with reduced drinking water owing to drought from 1991 to 2018.

Based on the analysis of the real contour map of the wavelet coefficient of the number of people with reduced drinking water owing to drought in China from 1991 to 2018 (see Figure 9), the figure clearly shows the fluctuation characteristics of the real part of the wavelet transform coefficients. This was reflected in the alternating characteristics of varying numbers of people with reduced drinking water owing to drought.

The scale fluctuations at approximately 10 a, 17 a, and 50 a were obvious, and the positive and negative phases appeared alternately. Obviously, in the calculation time domain, there were more and fewer population fluctuations in the number of people below. There were 35–50 years and 5–17 years of change in the evolution of the country's population with reduced drinking water owing to drought from 1991 to 2018. Among them, the number of quasi-second earthquakes in the 35–50 years were in 2002 and 2018. There were three quasi-shocks in the 5–17 year cycle. There were two more centres and two fewer centres over the entire time scale, which were in 1993, 2002, 1999, and 2018, respectively. At the 35–50 year time scale, there was one more obvious centre and one less obvious centre in 2002 and 2018, respectively. At the 5–17 year time scale, there were three periodic oscillation centres. In 1993, 2011, and 1999, there were two more centres and one less centre.

3.3.5. Domestic Animals with Reduced Drinking Water Owing to Drought

By analysing the wavelet variance chart of the number of domestic animals with reduced drinking water owing to drought in China from 1991 to 2018 (see Figure 10), we can see that there were three more obvious peaks in the wavelet variance, corresponding to the times of 3, 16, and 50 years, respectively. Among them, the 50 year cycle had the largest variance value, which was the strongest in the period of approximately 50 years. This was the first main cycle of the annual change in the crop damage area in the country, the 16 year time scale was the second main cycle, and the 3 year time scale was the third main cycle.

By analysing the real part contour map of the wavelet coefficients of the number of domestic animals with reduced drinking water owing to drought from 1991 to 2018 in China (see Figure 11), we can see that the graph clearly shows the fluctuating characteristics of the real part of the wavelet transform coefficients, specifically in the alternating increases and decreases in the number of domestic animals with reduced drinking water owing to drought.

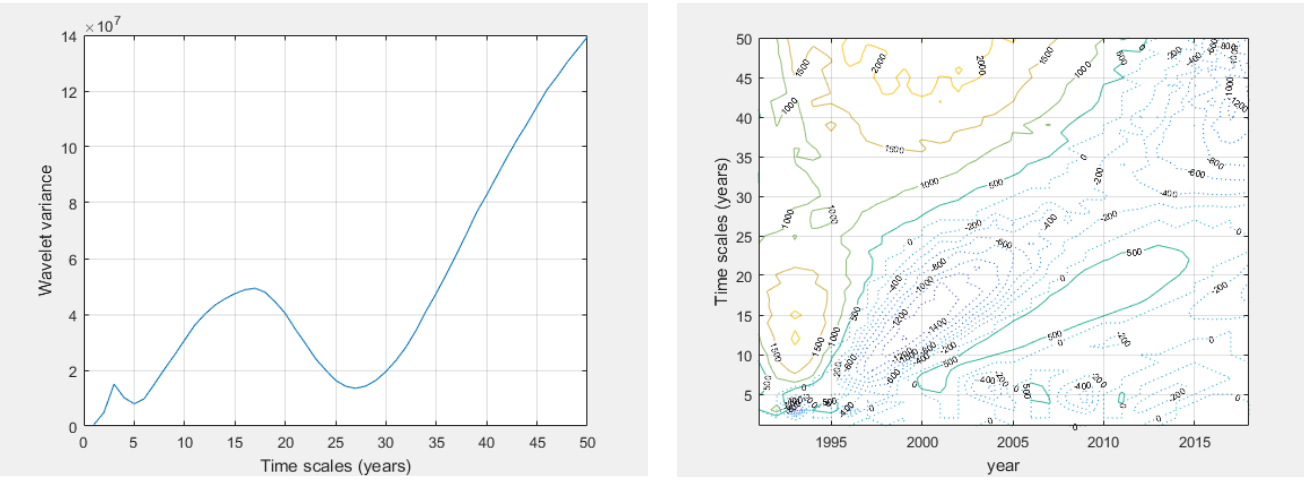

Figure 11. Wavelet variogram and coefficient real contours of the number of livestock with reduced drinking water owing to drought in China, 1991–2018.

The scale fluctuations at approximately 3a, 15a, and 50a were obvious, with the positive and negative phases appearing alternately. Obviously, in the calculation time domain, the number of domestic animals with reduced drinking water owing to drought fluctuated. From 1991 to 2018, there were 36–50 years and 7–21 years of changes in the number of domestic animals with reduced drinking water owing to drought. Among them, the number of quasi-two shocks that appeared alternately between 36 and 50 years was 2000 and 2018. In the period 7–21 years, there were two quasi-shocks. For the entire time period, there were two more centres and two fewer centres. At the time scale of 36–50 years, there was an obvious multicentre and a few centres in 2000 and 2018, respectively. At a time scale of 7–21 years, there were two periodic oscillation centres. In 1993 and 2000, there was one multi-centre and one fewer centre, respectively.

4. Discussion

4.1. Spatial and Temporal Distribution of Agricultural Weather Hazards in China and Future Outlook

This study first analysed the distribution trends and characteristics of agricultural disasters in Chinese provinces in recent years. Drought has become a global research concern. Several similar studies have been conducted in this regard [48]. Based on statistical data of drought and flood disaster areas and disaster areas in China from 1950 to 2010, Yao et al. found that the spatial distribution of drought disaster areas and disaster areas had different degrees of influence in various regions. The most severely affected area was north China, accounting for 11.09% of the country's disaster area [49]. This is consistent with the results of this study, which used statistical data from 1979 to 2008 to analyse the temporal change trends and spatial distribution characteristics of agricultural meteorological disasters in China over the past 30 years. Drought disasters were the most severe in north China, followed by the northeast and northwest, which is consistent with this study's results [50]. Others used statistical and comprehensive analysis methods to analyse the trends and causes of major meteorological disasters affecting agricultural production in China from 1995 to 2014. The overall trend declined, which was consistent with the results of this study [51]. Most of the previous research has focused on drought studies on a small scale, such as a province or a small area in the country, and there are few studies on the overall spatial distribution of drought disasters in various provinces throughout the country, but they also all prove that the number of drought disasters in China in recent years has decreased, and some drought prevention and control measures have contributed to good results. Severe agricultural drought in China was mainly located in the north, east, northeast, and southwest of China in 2000 and 2018, and both the worst and lightest droughts since the founding of new China. In addition to the M-K trend analysis, this study also used wavelet analysis to analyse agricultural drought disasters in the country over the past 30 years, deeply studying their trends, extreme years, and predictive roles in subsequent agricultural drought disaster research [52]. This study is of guiding significance for further understanding of the national spatial and temporal distributions of agricultural meteorological disasters and future trends, as well as for more scientific and effective strengthening of early warning and treatment measures for agricultural meteorological disasters. Simultaneously, we also found some measures and policies in recent years, such as the scientific implementation of the project of returning farmland to forests (grass and lakes) [53], scientifically adjusting the layout of agricultural production, improving the meteorological early warning mechanism, and the construction of meteorological disaster prevention projects.

4.2. Analysis of Disaster Risk Characteristics

Over the past 50 years, China's average annual drought-affected drought area has reached 22.17 million hectares, affecting 590 million people, causing 2155 deaths, affecting a total of 54,640,500 hm^2 of crops, including 6,666,600 hm^2 of crop failure, resulting in direct economic losses totalling approximately CNY 538.133 billion [54]. Constrained by climatic conditions and socioeconomic development, population growth, rapid increase in water consumption for agriculture, industry, and urban living, coupled with the deterioration of the water environment and reduced water availability, the frequency of drought in China remains high, the affected area is large, and drought disasters are an aggravating trend [55,56].

4.3. Limitations of Drought Hazard Trends

The innovation of this study was not only the analysis and prediction of drought disaster trends in China in recent years, but also its focus on the provinces whose number of drought disasters significantly increased and decreased, the trend in drought disasters, the causes of drought, the degree of drought, the various losses caused by drought, the preventive measures taken, and the effectiveness of the preventive measures [57]. This study focused on the overall spatial distribution of drought disasters in all provinces of China and refined the research area. It not only studied drought disasters in China in a macro and comprehensive manner, but it also studied provincial drought disasters in a targeted manner, which no longer resembles the traditional one in which the research is limited to a certain area. The research content was more abundant and the research results were more representative. However, this study had some limitations. We found that although some provinces experienced drought, it did not cause serious damage to agriculture, which is a major reason for the province's adaptability to climate change and modern agricultural tools.

4.4. Sustainable Management of Water Resources in Arid Areas

Understanding the relative impacts of climate change and human activities on runoff changes is of great significance for the sustainable management of water resources in arid regions [58]. This study has not yet systematically analysed the specific causes of agricultural drought disasters. In recent years, in the context of global warming, for the study of drought disasters, more comprehensive factors should be considered in the future. Research should combine temperature [59,60], precipitation, disaster-causing factors, disaster conditions, disaster-preventing environments, and human adaptability. In the future, we will focus on the specific causes of drought disasters and make efforts to better prevent and control them [61].

5. Conclusions

Through analysis of the average five drought disaster indicators in provinces across the country, including the crop damage area, drought-affected area of crops, crop failure area, population with reduced drinking water caused by drought, and the number of domestic animals with reduced drinking water caused by drought, it can be concluded that the larger areas of the crop damage area and drought-affected area of crops were Heilongjiang Province and the Inner Mongolia Autonomous Region. The impact of the crop damage and crop disaster areas was prominently reflected in 2007 and 2009. In recent years, crop failure has occurred in Inner Mongolia. The crops with the greatest impact on the crop failure area were in the Heilongjiang, Jilin, Liaoning, Hebei, Yunnan, and Guizhou provinces. The impact of drought disasters on the crop failure area was prominently reflected in 2007. In recent years, the number of people and domestic animals with reduced drinking water caused by drought were mainly reflected in Yunnan, Sichuan, Guizhou, Chongqing, Inner Mongolia, and other provinces (autonomous regions and municipalities), which were highlighted in 2006, 2009, and 2010.

In the M-K trend test, by analysing the Z-values of the five drought hazard indices, the overall trend decreased and in fewer individual provinces in northern and southern China. Among the other four indicators, except for Inner Mongolia, Tibet, Fujian, Anhui, Jiangsu, Shandong, and Henan provinces, all provinces showed a decreasing trend. Inner Mongolia passed the M-K trend test, reaching a significant level for the number of domestic animals that hade water difficulties caused by drought, showing a clear increasing trend. The remaining provinces passed the M-K test.

Wavelet analysis of the drought hazard index from 1991 to 2018 revealed that the scale of the fluctuation was very obvious. There was one more centre and one less centre during the whole time in 2002 and 2018, respectively. The number of people with reduced drinking water caused by drought had the strongest cyclical oscillations at approximately 10, 17, and 50 years. The scale fluctuations were obvious. Throughout the process, there were two major centres and two minor centres in 1993 and 2002, and in 1999 and 2018. In the country, the strongest cyclical oscillation in the number of domestic animals with reduced drinking water owing to drought was approximately 3, 16, and 50 years, and the scale fluctuations were very obvious.

The results of this study reveal the trends and distribution of drought hazards in China and contribute to a comprehensive understanding of changes in drought disasters. It can be concluded that agricultural drought disasters in China were the most severe in the northern region of the country. The crop damage areas, drought-affected areas, and crop failure areas in China were mainly distributed in the northern, eastern, northeastern, and southwestern regions of the country. People and domestic animals with reduced drinking water caused by drought were mainly concentrated in the northern and southwestern regions. Generally, the five drought indicators decreased. This indicates that some drought prevention measures played an important role.

Author Contributions: All authors contributed to this work. X.W., Writing—Original draft preparation and Conceptualisation; P.L., Writing—Review and editing; W.D., Methodology; Y.Z. (Yue Zheng), Visualisation; S.W., Software; W.Z., Visualisation; Y.Z. (Yuzhu Zhang) and D.N., Investigation and Supervision. All authors have read and agreed to the published version of the manuscript.

Funding: This study was supported by the Third Xinjiang Scientific Expedition Program (Grant No. 2022xjkk0107), the National Key R&D Program of China (2018YFE0103800), the International Education Research Program of Chang'an University (300108221102), the China National Social Science Fund Project (20XKS006), the Project of Ningxia Natural Science Foundation (2022AAC03700).

Data Availability Statement: The drought data in this study came from the drought disaster data in the "Bulletin of Flood and Drought Disaster in China" in recent years (http://www.mwr.gov.cn/sj/tjgb/zgshzhgb/ (accessed on 29 November 2022)) other data came from China Flood and Drought Disaster Bulletin.

Acknowledgments: This study was supported by the Third Xinjiang Scientific Expedition Program (Grant No. 2022xjkk0107), the China Scholarship Council (Grant No. Liujinmei (2022) No. 45; Liujinxuan (2022) No. 133; Liujinou[2023] No. 22), the Project of Ningxia Natural Science Foundation (2022AAC03700), the Youth Innovative Talents Program for Guangdong Universities in 2022 (2022KQNCX143), and the Yinshanbeilu Grassland Eco-Hydrology National Observation and Research Station, China Institute of Water Resources and Hydropower Research, Beijing 100038, China (Grant No. YSS2022004). We thank the reviewers for their valuable comments.

Conflicts of Interest: The authors declare no conflict of interest.

References

1. Mishra, A.K.; Singh, V.P. A review of drought concepts. *J. Hydrol.* **2010**, *391*, 202–216. [CrossRef]
2. Wang, J.; Yaohui, L.I.; Wang, R.; Feng, J.; Zhao, Y. Preliminary Analysis on the Demand and Review of Progress in the Field of Meteorological Drought Research. *J. Arid. Meteorol.* **2012**, *30*, 497.
3. Zhang, Z.G.; Hao, W.P.; Hao-Ru, L.I.; Mao, L.L.; Gao, X. Analysis on the Drought Characteristics in Different Growth Stages of Spring Maize in Shanxi Province. *Chin. J. Agrometeorol.* **2015**, *36*. [CrossRef]
4. Hao, L.; Joyeeta, G.; Pieter, V.D.M. China's Governance Structure on Drought Disaster in Rural Areas. *Disaster Adv.* **2012**, *5*, 976–980.
5. Yu, L.; Zhao, Y. Analysis of Drought-flood Disaster on Huanghuaihai Region During Summer Maize Growing Season. *J. Catastrophol.* **2013**, *28*, 71–75,80.
6. Li, X.; Li, D.; Wang, J. Spatiotemporal Characteristics of Droughtover China during 1961–2009. *J. Desert Res.* **2012**, *32*, 473–483.
7. Choi, M.; Jacobs, J.M.; Anderson, M.C.; Bosch, D.D. Evaluation of drought indices via remotely sensed data with hydrological variables. *J. Hydrol.* **2013**, *476*, 265–273. [CrossRef]
8. Liao, Y.; Zhang, C. Spatio-Temporal Distribution Characteristics and Disaster Change of Drought in China Based on Meteorological Drought Composite Index. *Meteorol. Mon.* **2017**, *43*, 1402–1409.
9. Begueria, S.; Vicente-Serrano, S.M.; Reig, F.; Latorre, B. Standardized precipitation evapotranspiration index (SPEI) revisited: Parameter fitting, evapotranspiration models, tools, datasets and drought monitoring. *Int. J. Climatol.* **2014**, *34*, 3001–3023. [CrossRef]
10. Jiao, W.; Zhang, L.; Chang, Q.; Fu, D.; Cen, Y.; Tong, Q. Evaluating an Enhanced Vegetation Condition Index (VCI) Based on VIUPD for Drought Monitoring in the Continental United States. *Remote Sens.* **2016**, *8*, 224. [CrossRef]
11. Moreira, E.E.; Coelho, C.A.; Paulo, A.A.; Pereira, L.S.; Mexia, J.T. SPI-based drought category prediction using loglinear models. *J. Hydrol.* **2008**, *354*, 116–130. [CrossRef]
12. Su, H.; Li, G. Low-frequency drought variability based on SPEI in association with climate indices in Beijing. *Acta Ecol. Sin.* **2012**, *32*, 5467–5475.
13. Du, H.; He, S. The Analysis on Characteristics of Precipitation and Trends in Drought and Flood Disasters in Minjiang River Basin. *Res. Soil Water Conserv.* **2015**, *22*, 153–157.
14. Duan, W.; Maskey, S.; Chaffe, P.L.B.; Luo, P.; He, B.; Wu, Y.; Hou, J. Recent Advancement in Remote Sensing Technology for Hydrology Analysis and Water Resources Management. *Remote Sens.* **2021**, *13*, 1097. [CrossRef]
15. Hu, G.U.O.; Ying, W.; Fang, W. Overview of Remote Sensing Approaches to Drought Monitoring. *Remote Sens. Technol. Appl.* **2008**, *23*, 111–116.
16. Liu, H.; Liu, R.; Liu, S. Review of Drought Monitoring by Remote Sensing. *J. Geo-Inf. Sci.* **2012**, *14*, 232–239. [CrossRef]
17. Luo, B.; Huang, W.; Shuai, X.; Xie, B.; Peng, L. Risk Division of Drought Disaster for Rice Production in Hunan Province. *Chin. J. Agrometeorol.* **2011**, *32*, 461–465.
18. Wang, M.; Yan, J. Precipitation Characteristics of Flooding from 1960 to 2012 and Serious Flooding Judgment for the Southeast Coast of China. *Earth Environ.* **2015**, *43*, 667–674.
19. Deng, H.; Pepin, N.C.; Chen, Y.; Guo, B.; Zhang, S.; Zhang, Y.; Chen, X.; Gao, L.; Meibing, L.; Ying, C. Dynamics of Diurnal Precipitation Differences and Their Spatial Variations in China. *J. Appl. Meteorol. Climatol.* **2022**, *61*, 1015–1027. [CrossRef]
20. Qin, J.; Duan, W.; Chen, Y.; Dukhovny, V.A.; Sorokin, D.; Li, Y.; Wang, X. Comprehensive evaluation and sustainable development of water-energy-food-ecology systems in Central Asia. *Renew. Sustain. Energy Rev.* **2022**, *157*. [CrossRef]

21. Tian, Z.; Li, X. Analysis on the trend of drought in main grain produCing areas in China from 1949 to 2016. *J. China Agric. Univ.* **2019**, *24*, 159–167.
22. Li, Z.; Niu, C.; Xia, J. Analysis on the Change of Precipitation in Multiple Temporal Scales in North China. *Arid Land Geogr.* **2004**, *27*, 548–552.
23. Duan, W.; Hanasaki, N.; Shiogama, H.; Chen, Y.; Zou, S.; Nover, D.; Zhou, B.; Wang, Y. Evaluation and Future Projection of Chinese Precipitation Extremes Using Large Ensemble High-Resolution Climate Simulations. *J. Clim.* **2019**, *32*, 2169–2183. [CrossRef]
24. Kumar, M.N.; Murthy, C.S.; Sai, M.V.R.S.; Roy, P.S. Spatiotemporal analysis of meteorological drought variability in the Indian region using standardized precipitation index. *Meteorol. Appl.* **2012**, *19*, 256–264. [CrossRef]
25. Zhiwei, W.; Panmao, Z.; Yongli, W.U. Analysis on Drought Variation over 10 Hydrological Regions in China during 1951–2005. *Plateau Meteorol.* **2007**, *26*, 874–880.
26. Yao, Y.; Zhang, Q.; Li, Y.; Wang, Y.; Wang, J. Drought Risk Assessment Technological Progresses and Problems. *Resour. Sci.* **2013**, *35*, 1884–1897.
27. Deng, Z.Y.; Zhang, Q.; Yin, X.Z.; Zhang, C.J.; Xin, J.W.; Liu, D.X.; Jin-Yong, P.U.; Dong, A.X. Response of Drought Damage to Arid Climate Change. *J. Glaciol. Geocryol.* **2007**, *29*, 114–118.
28. Zou, X.; Ren, G.; Zhang, Q. Droughts Variations in China Based on a Compound Index of Meteorological Drought. *Clim. Environ. Res.* **2010**, *15*, 371–378.
29. Zhou, Y.; Li, N.; Wu, J. Analysis of Drought and its Possible Causes in Inner Mongolia Region for Nearly 30 Years. *J. Catastrophol.* **2013**, *28*, 67–73.
30. Zhang, J. Risk assessment of drought disaster in the maize-growing region of Songliao Plain, China. *Agric. Ecosyst. Environ.* **2004**, *102*, 133–153. [CrossRef]
31. Ministry of Water Resources of the People's Republic of China. *Bulletin of Flood and Drought Disasters in China*; Ministry of Water Resources of the People's Republic of China: Beijing, China, 2012.
32. Mu, J.; Qiu, M.; Gu, Y.; Ren, J.; Liu, Y. Applicability of five drought indices for agricultural drought evaluation in Jilin Province, China. *Chin. J. Appl. Ecol.* **2018**, *29*, 2624–2632.
33. Hu, Z.; Liu, S.; Zhong, G.; Lin, H.; Zhou, Z. Modified Mann-Kendall trend test for hydrological time series under the scaling hypothesis and its application. *Hydrol. Sci. J.-J. Des Sci. Hydrol.* **2020**, *65*, 2419–2438. [CrossRef]
34. Anand, B.; Karunanidhi, D. Long term spatial and temporal rainfall trend analysis using GIS and statistical methods in Lower Bhavani basin, Tamil Nadu, India. *Indian J. Geo-Mar. Sci.* **2020**, *49*, 419–427.
35. Li, Q.; He, P.; He, Y.; Han, X.; Zeng, T.; Lu, G.; Wang, H. Investigation to the relation between meteorological drought and hydrological drought in the upper Shaying River Basin using wavelet analysis. *Atmos. Res.* **2020**, *234*, 104743. [CrossRef]
36. Li, X.; Yang, Y.; Ren, C. Some Key Problems in Palmer Index Analysis Using Wavelet Decomposition. *J. Shenyang Agric. Univ.* **2013**, *44*, 273–277.
37. Niu, C.; Zhang, L.; Xia, J. Wavelet Analysis on the Precipitation in North China. *Arid Land Geogr.* **2004**, *27*, 66–70.
38. Wang, W.; Ding, J.; Xiang, H. Application and prospect of wavelet analysis in hydrology. *Adv. Water Sci.* **2002**, *13*, 515–520.
39. Joshi, N.; Gupta, D.; Suryavanshi, S.; Adamowski, J.; Madramootoo, C.A. Analysis of trends and dominant periodicities in drought variables in India: A wavelet transform based approach. *Atmos. Res.* **2016**, *182*, 200–220. [CrossRef]
40. Song, X.; Wang, Y.; Yan, D.; Chen, Y.; Ding, Y. Fractal and wavelet analysis on the 59 years time series of drought disaster ratio in China. *Syst. Eng.-Theory Pract.* **2013**, *33*, 2986–2992.
41. Luo, P.; Liu, L.; Wang, S.; Ren, B.; He, B.; Nover, D. Influence assessment of new Inner Tube Porous Brick with absorbent concrete on urban floods control. Case Studies in Construction Materials **2022**, *17*, e01236.Huang, H. Characteristics and causes of drought in China from 1949 to 2007. *J. Arid Land Resour. Environ.* **2010**, *24*, 94–98.
42. Zhu, Y.; Luo, P.; Zhang, S.; Sun, B. Spatiotemporal Analysis of Hydrological Variations and Their Impacts on Vegetation in Semiarid Areas from Multiple Satellite Data. *Remote Sens.* **2020**, *12*, 4177. [CrossRef]
43. Luo, P.; Luo, M.; Li, F.; Qi, X.; Huo, A.; Wang, Z.; He, B.; Takara, K.; Nover, D.; Wang, Y. Urban flood numerical simulation: Research, methods and future perspectives. *Environ. Model. Softw.* **2022**, *156*. [CrossRef]
44. Hu, Y.; Duan, W.; Chen, Y.; Zou, S.; Kayumba, P.M.; Qin, J. Exploring the changes and driving forces of water footprint in Central Asia: A global trade assessment. *J. Clean. Prod.* **2022**, *375*, 134062. [CrossRef]
45. Wang, Z.; Luo, P.; Zha, X.; Xu, C.; Kang, S.; Zhou, M.; Nover, D.; Wang, Y. Overview assessment of risk evaluation and treatment technologies for heavy metal pollution of water and soil. *J. Clean. Prod.* **2022**, *379*, 134043. [CrossRef]
46. Zhao, Y.; Shi, X.; Wang, S.; Qin, N.; Wang, Q.; Feng, S. Research on Variations of Climate and Its Aridity in the Valley of Yellow River and Huangshui River within Qinghai Province. *J. Desert Res.* **2006**, *26*, 54–59.
47. Zhu, L.; Yan, J. A judgment of warming-drying climate changes and drought disaster trend of Xianyang City. *J. Arid Land Resour. Environ.* **2011**, *25*, 131–135.
48. Yao, Y.; Zheng, F.; Guan, Y. The temporal and spatial characteristics of flood and drought during the recent 60 years in China. *Agric. Res. Arid Areas* **2017**, *35*, 228–232,263.
49. Fang, S.; Yang, J.; Zhou, G. Change trend and distributive characteristics of agrometeorological disasters in China in recent 30 years. *J. Nat. Disasters* **2011**, *20*, 69–73.

50. Jiang, L.; Cui, X. Analysis on variation tendency and cause of China's agrometeorological hazards in the latest 20 years. *Torrential Rain Disasters* **2016**, *35*, 102–108.
51. Luo, P.; Mu, Y.; Wang, S.; Zhu, W.; Mishra, B.K.; Huo, A.; Zhou, M.; Lyu, J.; Hu, M.; Duan, W. Exploring sustainable solutions for the water environment in Chinese and Southeast Asian cities. *Ambio* **2021**, *51*, 1199–1218. [CrossRef]
52. Cao, Z.; Wang, S.; Luo, P.; Xie, D.; Zhu, W. Watershed Ecohydrological Processes in a Changing Environment: Opportunities and Challenges. *Water* **2022**, *14*, 1502. [CrossRef]
53. Guan, Y.; Wang, B.; Zheng, F.; Zhang, P.; Qin, C. Characteristics of meteorological disasters in China during 2012. *J. Nat. Disasters* **2014**, *23*, 24–31. [CrossRef]
54. Liu, Y.; Yang, Y. Spatial Distribution of Major Natural Disasters of China in Historical Period. *Acta Geogr. Sin.* **2012**, *67*, 291–300.
55. Yunfeng, C.; Ge, G.A.O. An Analysis to Losses Caused by Meteorological Disasters in China During 1989–2008. *Meteorol. Mon.* **2010**, *36*, 76–80.
56. Liu, Y.; Miao, Q. Prediction on Agricultural Drought Disasters in Northwest China. *Arid Land Geogr.* **2004**, *27*, 564–569.
57. Ye, X.; Liu, J.; Li, X.; Zhang, Q. Effects of climate variability and human activities on runoff variation of Ganjiang River Basin. *J. Hohai Univ. Nat. Sci.* **2013**, *41*, 196–203.
58. Limei, X.U.; Ying, G.U.O.; Min, L.I.U.; Qiaoli, H.U.; Fujun, C.; Shucong, Y.; Yanjun, S. Analysis of Temperature Trends and Change Points in the Haihe River Basin Over the Last 50 Years. *Resour. Sci.* **2011**, *33*, 995–1001.
59. Duan, W.; Zou, S.; Chen, Y.; Nover, D.; Fang, G.; Wang, Y. Sustainable water management for cross-border resources: The Balkhash Lake Basin of Central Asia, 1931–2015. *J. Clean. Prod.* **2020**, *263*. [CrossRef]
60. Bao, Y. Analysis of Urban Disaster Prevention and Mitigation. In Proceedings of the Advances in Civil Engineering, PTS 1-6, Xi'an, China, 22–24 September 2011; pp. 264–267.
61. Luo, P.; Zheng, Y.; Wang, Y.; Zhang, S.; Yu, W.; Zhu, X.; Huo, A.; Wang, Z.; He, B.; Nover, D. Comparative Assessment of Sponge City Constructing in Public Awareness, Xi'an, China. *Sustainability* **2022**, *14*, 11653. [CrossRef]